Journal of Marine Systems 88 (2011) 385–400

Contents lists available at ScienceDirect

Journal of Marine Systems

journal homepage: www.elsevier.com/locate/jmarsys

Environmental control of summer primary production in the Hudson Bay system: The role of stratification

Joannie Ferland [a,*], Michel Gosselin [a], Michel Starr [b]

[a] Institut des sciences de la mer (ISMER), Université du Québec à Rimouski, 310 Allée des Ursulines, Rimouski, Québec, Canada G5L 3A1
[b] Institut Maurice-Lamontagne, Pêches et Océans Canada, 850, route de la Mer, Mont-Joli, Québec, Canada G5H 3Z4

ARTICLE INFO

Article history:
Received 15 March 2010
Received in revised form 14 February 2011
Accepted 22 March 2011
Available online 13 April 2011

Keywords:
Primary production
Phytoplankton
Chlorophyll *a* biomass
Stratification
Carbon export
Hudson Bay

ABSTRACT

The influence of environmental factors on size-fractionated phytoplankton production and biomass (chlorophyll *a*) and community composition was examined in the Hudson Bay system (Hudson Bay, Hudson Strait, and Foxe Basin; HBS) during August 2004 and September 2005 and 2006. Significant variability in the vertical structure of the water column and melt season length was observed between years and between regions of the HBS. Even though there was no year-to-year variability in the phytoplankton production and biomass, we observed significant differences in the phytoplankton size structure and taxonomic composition between mid and late summer. For all years, phytoplankton production and biomass were lower in Hudson Bay (51–1217 mg C m^{-2} d^{-1}; 11–57 mg chl *a* m^{-2}) than in Hudson Strait (675–2740 mg C m^{-2} d^{-1}; 28–97 mg chl *a* m^{-2}). Negative correlation between primary production and stratification strength of the upper water column suggested nutrient limited primary production in Hudson Bay and the south shore of Hudson Strait. Stratification and nitrate concentration also explained the variability in the physiological state (i.e., production:biomass ratio) and size structure of phytoplankton communities between mid and late summer. Daily estimated summer primary production averaged 0.32 g C m^{-2} in Hudson Bay and 1.34 g C m^{-2} in Hudson Strait. Phytoplankton production in the HBS was largely dominated by ultraphytoplankton. On average, only ca. 30% of total production was potentially exported from the euphotic zone. The dominance of flagellate-dominated community may explain the low export of matter and energy toward deeper waters and likely toward the upper trophic levels.

1. Introduction

Primary production plays a central role in the oceans by supplying organic matter to higher trophic levels, including invertebrates, fishes, and marine mammals. Marine ecosystems in polar regions are particularly sensitive to changes in primary production due to their low number of trophic links (Grebmeier et al., 2006; Moline et al., 2008; Post et al., 2009). Phytoplankton also plays a key role in ocean biogeochemistry since it participates in the transformation of anthropogenic atmospheric CO_2 emissions into organic carbon via the biological pump. Thus any modification in phytoplankton production or community will greatly influence how the ocean will respond to climate change.

The Arctic domain is predicted to experience the most severe climate change (ACIA, 2005; IPCC, 2007; Walsh, 2009). Its sea-ice cover is shrinking faster than predicted (Comiso and Nishio, 2008; Johannessen et al., 2004; Kwok et al., 2009; Stroeve et al., 2007) and is expected to become solely a seasonal feature by mid-century (Wang and Overland, 2009). Intensification of the hydrological cycle is also predicted to occur due to increasing precipitation at high latitudes, increasing river discharge, and net melting of ice stocks on land and sea (McClelland et al., 2006; Peterson et al., 2006; Ziegler et al., 2003). The most striking effects of these changes for arctic primary producers will be the increase in both summer stratification and light availability.

Light and nutrient availability, to a large extent, dictate the amount and diversity of primary producers in the oceanic ecosystem (Mann and Lazier, 1996). Both factors have been found to limit primary production in the Arctic and sub-Arctic seas (Sakshaug, 2004). In polar ecosystems, sea-ice coverage limits the length of the productive season (Arrigo et al., 2008) in controlling the photosynthetic light requirement. Nonetheless, in coastal regions characterized by high freshwater discharge, stratification controls the level of primary production by limiting fluxes from the nutrient-rich deeper waters (Arrigo et al., 1999; Carmack, 2007; Smetacek and Nicol, 2005). The Hudson Bay system (HBS) is the largest northern inland sea in the world and includes three different hydrographic regions (i.e., a strait, a bay, and a basin) characterized by contrasting ice coverage, water-column stratification, and water depth (Harvey et al., 2001, 2006; Saucier et al., 2004). It also receives input from the largest watershed in North America and Eurasia (Shiklomanov et al., 2000) totaling

* Corresponding author. Tel.: +1 418 723 1986x1761; fax: +1 418 724 1842.
E-mail addresses: joannie.ferland@takuvik.ulaval.ca (J. Ferland), michel_gosselin@uqar.qc.ca (M. Gosselin), michel.starr@dfo-mpo.gc.ca (M. Starr).

0924-7963/$ – see front matter © 2011 Elsevier B.V. All rights reserved.
doi:10.1016/j.jmarsys.2011.03.015

717 km^3 freshwater per year (Déry et al., 2005). Freshwater stratification has already been identified as being perhaps the most important factor governing ocean climate, nutrient fluxes and biologigal productivity of the HBS (Drinkwater and Jones, 1987; Prinsenberg, 1977).

Primary production and its relationships with water mass characteristics have occasionally been examined in Hudson Bay (Grainger, 1982; Jones and Anderson, 1994; Legendre and Simard, 1979) but never been studied simultaneously in the three HBS hydrographic regions. The only phytoplankton production measurements in HBS were conducted near Belcher Island in June–July 1958 and July–September 1959 (Grainger, 1982), in southeastern Hudson Bay in August–September 1976 (Legendre and Simard, 1979), and in northern Foxe Basin in August–September 1981 (Smith et al., 1985; Subba Rao and Platt, 1984). These studies reported low summer primary production (i.e., <3.5 mg C m^{-3} h^{-1} in the upper 20 m of the Bay and 0.2 g C m^{-2} d^{-1} in northern Foxe Basin). Based on these limited data, the annual primary production has been estimated at 35–70 g C m^{-2} (Roff and Legendre, 1986; Sakshaug, 2004) in Hudson Bay and at 24 g C m^{-2} in northern Foxe Basin (Subba Rao and Platt, 1984). These values are comparable to other oligotrophic Arctic shelves (20–70 g C m^{-2} yr^{-1}) and much lower than productive Arctic shelves and the Atlantic sector of the Arctic Ocean (60–400 g C m^{-2} yr^{-1}; Sakshaug, 2004). To our knowledge, no primary production rate has been published for Hudson Strait and southern Foxe Basin.

In contrast to primary production, surface chlorophyll *a* (chl *a*) distribution has been well studied in Hudson Bay and Hudson Strait (Anderson and Roff, 1980a; Drinkwater and Jones, 1987; Harvey et al., 1997). The surface waters of Hudson Bay showed higher chl *a* concentrations inshore than offshore (Anderson and Roff, 1980a) and lower values than in Hudson Strait (Drinkwater and Jones, 1987; Harvey et al., 1997). These earlier studies suggested enhanced primary productivity in areas of strong tidal mixing, where nutrient concentrations are periodically replenished.

The aims of this study were (1) to describe the variability in the production and biomass of small (0.7–5 μm) and large (>5 μm) phytoplankton across three contrasted hydrographic regions of the Hudson Bay system (i.e., northern Hudson Bay, Hudson Strait, and southern Foxe Basin) during the summers of 2004, 2005, and 2006, (2) to assess the roles of the various environmental factors, notably stratification, on the variability of primary production, and (3) to determine the potential fate of phytoplankton carbon. This study will allow us to test the hypothesis of Drinkwater and Jones (1987), which is that primary production in the Hudson Bay system is governed by the vertical stability of the water column. The hypothesis that highly stratified, nutrient-poor waters are dominated by small phytoplankton cells exporting a small amount of carbon to deep waters (Legendre and LeFèvre, 1989) will also be tested.

2. Methods

2.1. Study area

Hudson Bay together with Foxe Basin and Hudson Strait (hereafter referred to as the Hudson Bay system, HBS) forms the world's largest inland sea (Prinsenberg, 1984), with an area of 1.24×10^6 km^2 (Saucier et al., 2004). Both Hudson Bay and Foxe Basin are shallow seas, averaging, respectively, 125 and 100 m and not exceeding 300 m in depth. Hudson Bay and Foxe Basin connect with the Labrador Sea (Atlantic) by way of the dynamic Hudson Strait and with the Arctic Ocean through Fury and Hecla Strait (Fig. 1). In contrast to the Bay, Hudson Strait is a deep (ca. 400 m) and wide (ca. 150 km) channel. It is recognized as an area of intense mixing driven by three major surface currents (Drinkwater, 1986, 1990): (1) a weaker (10–20 cm s^{-1}) flow of Labrador Sea (Atlantic) water inflowing northwestward, (2) a more intense (30–40 cm s^{-1}) flow of water from Foxe Basin and Hudson Bay outflowing southeastward, and (3) a strong cross-channel flow in the eastern half of the Strait. Strong tidal currents enhance the mixing, affecting vertical stratification of the water column, surface nutrient concentrations, and biological production processes in the area (Drinkwater, 1986, 1990).

Climate in the HBS is abnormally cold relative to other oceanographic systems at similar latitudes, such as the Bering and Baltic seas. The HBS is generally completely ice covered from January until April with occasional ice leads along the western coast of Hudson Bay and around the Belcher Islands. From May to mid-August, the ice cover breaks up starting with the eastern and western coastal areas of Hudson Bay. Open-water areas then expand so that by August, the remnant ice cover is found in the southeastern area of Hudson Bay and in Foxe Basin. The HBS is usually ice-free beginning in early August and starts to freeze up in mid-October, starting from the northwestern area of Foxe Basin and around Southampton Island, after which it generally spreads southwards (Saucier et al., 2004; Canadian Ice Service, Environment Canada, 2009; Hochheim and Barber, 2010; Hochheim et al., 2011).

Another striking feature of the HBS is its immense catchment area (3.1×10^6 km^2), which is one-third of Canada's watershed (Prinsenberg, 1980). Total river discharge into HBS (717 km^3 yr^{-1}, McClelland et al., 2006) is over twice that of either the St. Lawrence or Mackenzie river systems. Every year, runoff and melting ice create a 64 cm layer of freshwater in Hudson Bay (Steward and Lockhart, 2005), building up strong year-round stratification. This large freshwater intrusion follows a cyclonic surface circulation of about 5 cm s^{-1} (Prinsenberg, 1986). The deep water of arctic origin flows in the same direction but much more slowly. Barber (1967) and Prinsenberg (1986) measured winter mixing of 50–75 m and 90 m in depth, respectively. This means that the vertical mixing between surface and deep-water layers is incomplete throughout the year (Roff and Legendre, 1986).

2.2. Sampling

Sampling was conducted from 2 to 15 August 2004, from 1 to 10 September 2005, and from 30 August to 10 September 2006 onboard the icebreaker CCGS *Pierre Radisson*. Samples were collected at six stations along a longitudinal transect of ca. 700 km in northern Hudson Bay (ca. 60°N), at one station in Foxe Basin, and at 4 to 15 stations in Hudson Strait (Fig. 1). At sampling stations, water depths averaged 156 m in Hudson Bay, 377 m in Foxe Basin and 237 m in Hudson Strait. These expeditions were part of the MERICA-nord program (Étude des mers intérieures du Canada/Canadian Inland Sea study) of the Department of Fisheries and Oceans Canada. The aim of this project was to detect, understand, and predict climate change and variability in the HBS (Harvey et al., 2006).

During each expedition, incident downwelling irradiance (photosynthetically active radiation, PAR, 400–700 nm) was recorded at 2–10 min intervals on deck with a Li-COR 2 π quantum sensor (LI-190 SA). At each station, sea-ice coverage was estimated visually. A rosette sampling unit equipped with a CTD (conductivity–temperature–depth) probe (Sea-Bird Electronics SBE 911+), an underwater PAR sensor (Biospherical QSP-2200 Scalar), an in situ fluorometer (WETStar mini fluorometer model 9512008), and 12 ten liter Niskin bottles were deployed to obtain water temperature, salinity, density (sigma-*t*, σ_t), irradiance, and chlorophyll fluorescence down to about 10 m above the bottom. The diffuse light attenuation coefficient (K_d, m^{-1}) in the euphotic zone was determined by the slope of a linear regression between the natural logarithm of underwater PAR and depth, and when not possible, from the Secchi disk depth using the conversion factor of 1.44 (Holmes, 1970). The euphotic zone (Z_{eu}) was defined as the depth receiving 0.2% of the surface PAR (Knap et al., 1996). Water samples were collected at 6–7 discrete optical depths

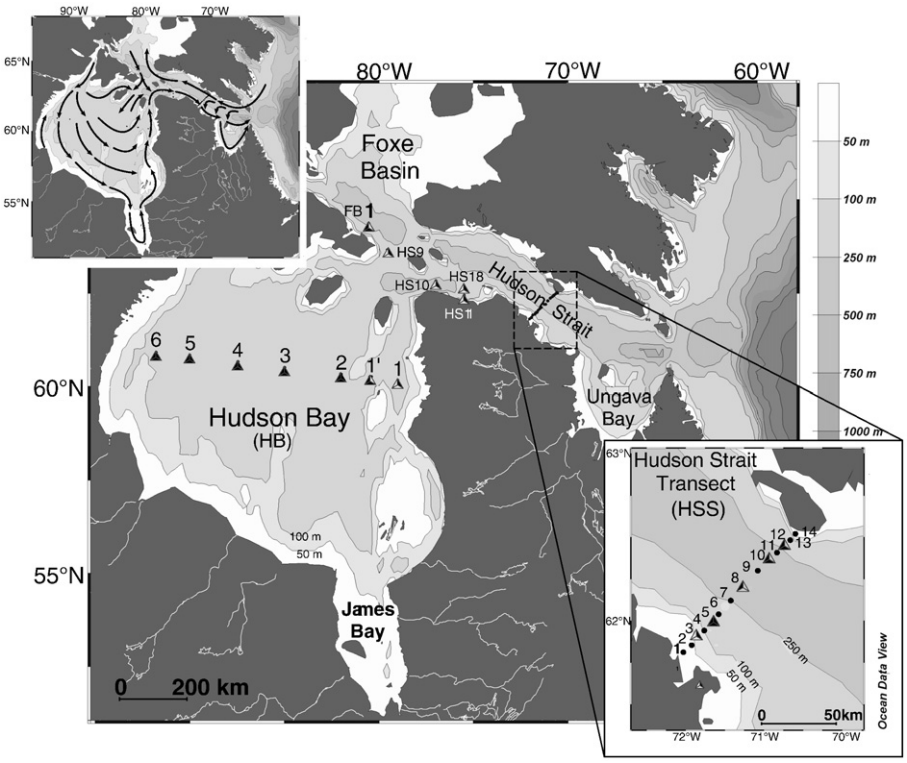

Fig. 1. Locations of the sampling stations in the Hudson Bay system during the summers of 2004 (▲), 2005 (▲), and 2006 (▲). Rivers with a discharge ≥14 $km^3 yr^{-1}$ are shown (Déry et al., 2005). In the upper map, the arrows indicate the summer surface circulation pattern (adapted from Drinkwater, 1986; Prinsenberg, 1986). In the lower map, the circles show the location of CTD stations where there was no chemical or biological sampling.

(100, 50, 30, 15, 5, 1, and 0.2% of surface PAR), including the depth of maximum chlorophyll fluorescence (DCM), and at 2–4 depths between the base of Z_{eu} and ca. 120 m. Subsamples for subsequent analyses were drawn from the Niskin bottles into acid-washed Nalgene bottles (Knap et al., 1996).

2.3. Laboratory analyses

Samples for dissolved inorganic nutrients were filtered through precombusted (450 °C for 5 h) Whatman GF/F glass fiber filters (nominal pore size of 0.7 μm) and the filtrated water collected in 5 ml acid-washed polycarbonate cryovials. Nutrient samples were then stored in a −80 °C freezer for later analyses of nitrate plus nitrite ($NO_3 + NO_2$), nitrite (NO_2), phosphate (PO_4), and silicic acid ($Si(OH)_4$) with a Technicon II autoanalyzer (Mitchell et al., 2002).

Samples for the identification and enumeration of phytoplankton cells >4 μm were collected at the DCM. They were preserved in acidic Lugol's solution (Parsons et al., 1984) and stored in the dark at 4 °C until analysis. Cells were identified following the inverted microscope method (Lund et al., 1958).

For size-fractionated chl *a* determination, two 500 ml subsamples were filtered through 25 mm Whatman GF/F fiber glass filters (total phytoplankton biomass: B_T, ≥0.7 μm) and two others through 25 mm Poretics 5 μm polycarbonate membrane filters (biomass of large phytoplankton: B_L, ≥5 μm). Concentrations of chl *a* were measured on board the ship with a Turner Designs TD-700 fluorometer after 18 h of pigment extraction in 90% acetone at 4 °C in the dark (acidification method of Parsons et al., 1984). The biomass of small phytoplankton cells (B_S, 0.7–5 μm) was obtained by subtracting B_L from B_T. Pheopigment concentrations were also determined after acidification of the extracted pigments with 50 μl of 5% HCl (Parsons et al., 1984).

Primary production rates were measured at the 6–7 sampled optical depths using the ^{14}C assimilation method (Knap et al., 1996; Pommier et al., 2009). Two light and one dark 500 ml Nalgene polycarbonate bottles were filled with seawater from each light level and then inoculated with 20 μCi of $NaH^{14}CO_3$. The dark bottle containing 200 μl of 0.02 mol l^{-1} 3-(3,4-dichlorophenyl-1,1)-dimethylurea (DCMU) was used to determine ^{14}C uptake rates not associated with photosynthetic processes (Legendre et al., 1983). The total amount of radioisotope in three randomly selected bottles was determined immediately after inoculation by pipetting 50 μl subsamples into 10 ml of Ecolume scintillation cocktail (ICN™) containing 50 μl of ethanolamine (Sigma). Bottles containing the ^{14}C isotope were incubated for 24 h in a Plexiglas deck incubator set up on a black board and equipped with tubes wrapped with neutral density screens (LEE Filters) to simulate irradiance at the seven sample collection depths. Tubes simulating ≤30% PAR were wrapped with one layer of blue filter to mimic vertical changes in spectral quality (Smith et al., 1997). Running seawater pumped from a depth of about 5 m from the surface circulated through the incubator to maintain the temperature at that of surface mixed layer. Incubations were initiated when possible in the morning (minimal PAR) or at dawn, depending on transits and overall sampling logistics, in order to reduce variability in ^{14}C accumulation (Mingelbier et al., 1994). Water temperature within the incubator was measured regularly during the incubation. In 2004 and 2005, after incubation, a 4 ml subsample was taken from each bottle and poured into borosilicate scintillation vials, acidified with 500 μl of 6 N HCl, and left open on a lab rotator in a fume hood for at least 4 h to release inorganic carbon prior to the measurement of total organic carbon production (P_{TOC}). The same treatment was also applied to another 4 ml subsample that was filtered through a Millex-DV syringe-driven filter unit (0.22 μm pore size) to measure the release rate of dissolved organic carbon (P_{DOC}). P_{TOC} and P_{DOC} samples were then neutralized with 500 μl of 6 N NaOH before adding 15 ml of scintillation cocktail. Total particulate organic carbon production (P_T) was measured from a 250 ml subsample filtered on Whatman GF/F filters. The remaining subsamples were filtered on Poretics 5 μm polycarbonate membrane filters to measure the fraction of the production by large phytoplankton

(P_L, ≥5 μm). The filters were rinsed with filtered seawater before being removed from the filtration system and placed in borosilicate scintillation vials. Filters were then acidified with 200 μl 0.5 N HCl and left to evaporate overnight on a lab rotator in a fume hood to remove any ^{14}C that had not been incorporated (Lean and Burnison, 1979). Once the filter was dried, 10 ml of scintillation cocktail was added to vials. Vials were stored in a dry and dark room for later counting (within two months) with a Beckman LS 6500 liquid scintillation counter. Production rates of particulate and dissolved organic carbon were calculated according to Parsons et al. (1984) using a factor of 1.05 to correct for the lower uptake of ^{14}C compared to ^{12}C (Knap et al., 1996). Values from the dark bottles were subtracted from corresponding light values based on the premise that the measured dark fixation of ^{14}C is due solely to bacterial processes occurring similarly in light and in dark bottles (Li et al., 1993). In 2004, primary production rates at 0.2% surface irradiance were set to 0 mg C m^{-3} d^{-1} since they were not measured. Production of the small phytoplankton (P_S, 0.7–5 μm) was obtained by subtracting P_L from P_T. The percent release of DOC during incubation was calculated as P_{DOC}:P_{TOC} multiplied by 100. This method provides conservative estimates of net primary production.

2.4. Calculations

Ice break-up dates (here defined as 80% ice coverage) at each station were estimated from Nimbus-7 SMMR and DMSP SSM/I passive microwave data provided by the National Snow and Ice Data Center (Cavalieri et al., 1996). Ice coverage values were extracted from the cell (ca. 25 km^2) nearest to the geographic coordinates of the sampling stations. For each sampled year, we calculated the number of open-water (<80% sea-ice coverage) days prior to sampling (OWDPS).

Water temperature, salinity, and density (σ_t) were averaged over 1 db intervals (ca. 1 m). The surface mixed layer depth (Z_m) was determined as the depth of the shallowest extreme curvature of the σ_t profile (adapted from Lorbacher et al., 2006) whereas the nutricline depth (Z_{nutr}) was estimated to be where the vertical gradient in NO_3 concentration (dNO_3^-/dz) was highest. Daily irradiance (E) averaged over Z_{eu} ($E_{0\text{-}Zeu}$) and Z_m ($E_{0\text{-}Zm}$) was calculated using the equation of Riley (1957):

$$E = E_0\left(1-e^{-Kd*Z}\right) / K_d*Z \quad (1)$$

where E_0 is the incident irradiance (E m^{-2} d^{-1}) and Z is either Z_m or Z_{eu} (m). The freshwater content (FWC; expressed in meters) was determined as the integrated salinity fraction above 34.8 salinity (Aagaard and Carmack, 1989; Melling et al., 2008):

$$FWC = \int_{0-i\ m}(S-34.8) / 34.8*dz \quad (2)$$

where dz is the vertical thickness, i stands for Z_m, and S is the mean salinity for the layer. The strength of the vertical stratification was estimated using two different indices: (1) the difference in σ_t between 80 and 5 m ($\Delta\sigma_t$) and (2) the Brunt–Väisälä frequency (N^2) (Tritton, 1988). There was a strong linear relationship between the stratification index determined by $\Delta\sigma_t$ and N^2 ($r^2 = 0.97$, $p < 0.0001$). Therefore, only $\Delta\sigma_t$ was considered in further analysis.

Temperature and salinity were averaged over Z_{eu} ($T_{0\text{–}Zeu}$, $S_{0\text{–}Zeu}$) and Z_m ($T_{0\text{–}Zm}$, $S_{0\text{–}Zm}$). Concentrations of nutrients and chl *a* were integrated over Z_{eu} and Z_m and primary production over Z_{eu} using trapezoidal integration (Knap et al., 1996). Mean integrated values were obtained by dividing the depth-integrated values by the integration depth.

2.5. Statistical analyses

Two-way analyses of variance (ANOVA) were used to test the difference in the mean value of each variable between sampling years (i.e., 2004, 2005, and 2006) and sampling regions (i.e., Hudson Bay, Foxe Basin, and Hudson Strait). One-way ANOVAs were then run to seek differences in the mean values of each variable between sampling years or sampling regions (Sokal and Rohlf, 1995). Before undertaking the ANOVAs, each variable's normality of distribution and homogeneity of variance were tested with Shapiro–Wilk and Levene tests, respectively. When required, data were log-transformed. ANOVAs were completed by a multiple comparison test of mean (Tukey's Honesty Significant Difference test for unequal sample sizes). A principal component analysis (PCA) was performed to explore the relationships between environmental factors (i.e., Z_m, Z_{eu}, Z_{nutr}, $\Delta\sigma_t$, $E_{0\text{–}Zeu}$, $T_{0\text{–}Zeu}$, $NO_3 + NO_{2(0\text{–}Zeu)}$, OWDPS) and total particulate phytoplankton production (P_T) and total chl *a* biomass (B_T). Pearson's correlations and simple regressions (model II, reduced major axis) were used to determine the linear relationship between two variables (Sokal and Rohlf, 1995). Statistical tests were performed with the SAS 9.2 software. Contour plots were drawn using the ODV 3.4.1 software (Schlitzer, 2004).

3. Results

Two-way analyses of variance revealed that several variables showed significant differences both between regions and sampling

Table 1
Environmental conditions (mean ± standard error) in the three regions of the Hudson Bay system during the summers of 2004 to 2006. Latest ice break-up date; $E_{(0\text{–}Zeu)}$: mean irradiance in the euphotic zone (Z_{eu}); $\Delta\sigma_T$: mean column stratification index; $T_{(0\text{–}Zeu)}$ and $T_{(0\text{–}Zm)}$: mean temperature in Z_{eu} and in the surface mixed layer (Z_m), respectively; $S_{(0\text{–}Zeu)}$ and $S_{(0\text{–}Zm)}$: mean salinity in Z_{eu} and in Z_m, respectively; FWC: freshwater content in Z_m (reference salinity = 34.8).

HBS region	Break-up date (<80% sea ice coverage)	$E_{(0\text{–}Zeu)}$ (E m^{-2} d^{-1})	$\Delta\sigma_T$	$T_{(0\text{–}Zeu)}$ (°C)	$S_{(0\text{–}Zeu)}$	$T_{(0\text{–}Zm)}$ (°C)	$S_{(0\text{–}Zm)}$	FWC (m)
2004								
Hudson Bay	02 Jul	6.5 ± 1.5	3.6 ± 1.0	0.7 ± 1.7	31.0 ± 1.2	5.0 ± 12.8	29.3 ± 1.6	5.6 ± 1.6
Foxe Basin	29 Jun	2.3	3.0	−0.7	32.2	2.8	29.7	5.2
Hudson Strait	15 Jun	6.3 ± 0.9	1.8 ± 0.4	1.5 ± 0.9	30.9 ± 0.3	2.7 ± 1.1	30.7 ± 0.5	4.2 ± 0.5
2005								
Hudson Bay	17 Jun	2.9 ± 1.4	4.6 ± 1.1	2.0 ± 0.6	30.8 ± 0.9	9.3 ± 1.2	28.4 ± 1.3	6.5 ± 1.3
Foxe Basin	17 Jun	4.0	1.8	0.5	31.8	2.9	31.0	3.8
Hudson Strait	13 Jun	2.6 ± 0.7	0.9 ± 0.5	1.9 ± 0.6	32.2 ± 0.7	2.8 ± 0.7	31.6 ± 0.9	3.3 ± 1.1
2006								
Hudson Bay	07 Jun	3.6 ± 0.4	3.2 ± 0.3	2.4 ± 1.5	31.1 ± 0.8	8.2 ± 0.4	29.9 ± 0.4	5.0 ± 0.4
Foxe Basin	07 Jun	2.2	0.6	1.9	32.6	2.9	32.4	2.4
Hudson Strait	10 May	3.6 ± 1.4	0.9 ± 0.2	2.4 ± 0.7	32.2 ± 0.6	4.2 ± 0.7	32.0 ± 0.5	2.8 ± 0.5

Table 2
Key depths (mean ± standard error) in the three regions of the Hudson Bay system during the summers of 2004 to 2006. Z_m: surface mixed layer depth; Z_{nutr}: nutricline depth; Z_{eu}: euphotic zone depth.

HBS region	Z_m (m)	Z_{nutr} (m)	Z_{eu} (m)
2004			
Hudson Bay	11 ± 4	45 ± 7	48 ± 11
Foxe Basin	6	49	55
Hudson Strait	8 ± 3	37 ± 13	28 ± 3
2005			
Hudson Bay	14 ± 2	45 ± 9	55 ± 6
Foxe Basin	19	57	56
Hudson Strait	18 ± 3	34 ± 13	37 ± 10
2006			
Hudson Bay	21 ± 7	51 ± 11	64 ± 16
Foxe Basin	35	48	57
Hudson Strait	18 ± 3	32 ± 10	48 ± 9

years (i.e., OWDPS, $\Delta\sigma_t$, FWC, Z_m, $Si(OH)_{4(0–Zeu)}$, and B_s), whereas some variables showed differences only between regions (i.e., Z_{eu}, Z_{nutr}, B_T, B_L, P_T, P_L, and P_S) or only between sampling years (i.e., $E_{0–Zeu}$, $NO_3 + NO_{2(0–Zeu)}$, $NO_3 + NO_{2(0–Zm)}$, and $PO_{4(0–Zeu)}$) (see mean values in Tables 1, 2, and 3).

3.1. Physical environment

In August 2004 and September 2005 and 2006, all sampling stations were free of ice except station HS9, where ice coverage was ca. 30% in 2004. In the different regions of HBS, ice break-up occurred at different dates during the three studied years (Table 1). In this study, we defined ice break-up as the earliest date when all stations of a given region were covered by <80% sea ice. The sea ice always retreated first from stations sampled in Hudson Strait, then the melting spread to the Hudson Bay and Foxe Basin stations (Table 1). For all regions, the earliest break-up occurred in 2006 and the latest in 2004. During this study, the mean duration of day length was ca. 16 h in 2004 and ca. 14 h in 2005 and 2006.

During the three sampling years, sea-surface temperature (SST) and salinity (SSS) varied spatially in the HBS (Figs. 2–4, Table 1). SST averaged 8.1 ± 0.4 °C in Hudson Bay, with a minimum of 3 °C in August 2004. SST in Hudson Strait was colder, averaging 3.4 ± 0.4 °C, with a minimum of 1.1 °C in 2004. The lowest SST was recorded in Foxe Basin, with a mean of 2.7 ± 0.2 °C. For all sampling years, Hudson Bay had the freshest surface water (mean SSS of 29 ± 0.3) compared to Hudson Strait (mean SSS of 31.5 ± 0.2) and Foxe Basin (mean SSS of 31 ± 0.8). Fresher and warmer waters were particularly found on the eastern side of Hudson Bay and on the south shore of the Strait (Figs. 2–4). In Hudson Bay, the surface mixed layer was shallower and cooler by an average of 3.7 °C in 2004 compared to 2005 and 2006 (Tables 1 and 2). In Hudson Strait, Z_m was also shallower and cooler in 2004 than in 2006, by an average of 1.5 °C. As a whole, the HBS was more stratified in 2004 and 2005 than in 2006 (mean $\Delta\sigma_t$ of 3.0, 3.3, and 2.1, respectively). The upper water column was more stratified in Hudson Bay than in Foxe Basin and Hudson Strait (mean $\Delta\sigma_t$ of 3.8, 1.8, and 1.2, respectively). The euphotic zone was deeper in Hudson Bay and Foxe Basin than in Hudson Strait (mean Z_{eu} of 55, 56, and 38 m, respectively; Table 2). For all stations, the surface mixed layer was always shallower (<22 m) than the euphotic zone (>24 m) during the study period (Figs. 2–4).

3.2. Nutrients

In the summers of 2004, 2005, and 2006, mean integrated $NO_3 + NO_2$ concentrations in Z_{eu} (volumetric) ranged from 0.1 to 12.3 mmol m^{-3} in the HBS (weighted average of 1.09 mmol m^{-3}; Table 3, Figs. 2–4). Above the chl *a* maximum (Figs. 2–4), $NO_3 + NO_2$ concentrations were almost depleted (usually <1 mmol m^{-3}) at all stations. In the HBS, mean integrated PO_4 concentrations in Z_{eu} varied between 0.35 and 2.25 mmol m^{-3} (weighted average of 0.66 mmol m^{-3}; Table 3). In the HBS, $Si(OH)_4$ was the most abundant nutrient in the water during the study period, with mean integrated concentrations in Z_{eu} ranging from 0.1 to 24.4 mmol m^{-3} (weighted average of 3.3 mmol m^{-3}; Table 3). There was no consistent regional pattern in $NO_3 + NO_2$ and PO_4 concentrations, but the Bay showed higher $Si(OH)_4$ concentrations than Foxe Basin and Hudson Strait (Table 3). In contrast, the HBS showed year-to-year differences in nutrient inventories. The mean integrated $NO_3 + NO_2$, PO_4, and $Si(OH)_4$ concentrations in Z_{eu} were higher in 2004 than in 2006 (Table 3). The mean $(NO_3 + NO_2)$:$Si(OH)_4$ and $(NO_3 + NO_2)$:PO_4 atomic ratios in Z_{eu} were respectively 0.43 and 2.29 in Hudson Bay, 0.75 and 2.21 in Hudson Strait, and 1 and 1.53 in Foxe Basin. These values are lower than the Redfield ratios of 1:1 and 16:1 (Redfield et al., 1963), suggesting that dissolved inorganic nitrogen was the macronutrient in lowest supply for phytoplankton growth in the HBS.

The surface-to-bottom difference in nutrient inventory is generally recognized to be related to the strength of the water column stratification, which reduces vertical exchange processes (Mann and Lazier, 1996). Below 100 m, inorganic nutrient ($NO_3 + NO_2$, $Si(OH)_4$, and PO_4) concentrations remained high in Hudson Bay (data not shown). For the years sampled, the bottom water of Hudson Bay contained $NO_3 + NO_2$ concentrations ranging from 7 to 15 mmol m^{-3}, $Si(OH)_4$ from 16 to 46 mmol m^{-3}, and PO_4 from 1.3 to 2.1 mmol m^{-3}.

Table 3
Nutrient concentrations in the three regions of the Hudson Bay system during the summers of 2004 to 2006. Mean integrated values (± standard error) over the euphotic zone (Z_{eu}) and the surface mixed layer (Z_m) are given for nitrate plus nitrite ($NO_3 + NO_2$), nitrite (NO_2), phosphate (PO_4), and silicic acid ($Si(OH)_4$) concentrations.

HBS region	$NO_3 + NO_{2\ (0–Zeu)}$ (mmol m^{-3})	$NO_{2\ (0–Zeu)}$ (mmol m^{-3})	$PO_{4\ (0–Zeu)}$ (mmol m^{-3})	$Si(OH)_{4\ (0–Zeu)}$ (mmol m^{-3})	$NO_3 + NO_{2\ (0–Zm)}$ (mmol m^{-3})	$NO_{2\ (0–Zm)}$ (mmol m^{-3})	$PO_{4\ (0–Zm)}$ (mmol m^{-3})	$Si(OH)_{4\ (0–Zm)}$ (mmol m^{-3})
2004								
Hudson Bay	1.22 ± 1.00	0.08 ± 0.02	0.69 ± 0.09	3.82 ± 0.70	0.25 ± 0.14	0.06 ± 0.01	0.56 ± 0.06	3.67 ± 1.14
Foxe Basin	1.36	0.08	0.63	0.59	0.22	0.05	0.47	0.52
Hudson Strait	0.58 ± 0.32	0.07 ± 0.01	0.52 ± 0.04	2.38 ± 0.75	0.20 ± 0.05	0.06 ± 0.01	0.45 ± 0.05	1.30 ± 0.62
2005								
Hudson Bay	2.17 ± 1.88	0.09 ± 0.01	0.73 ± 0.16	4.88 ± 3.33	0.22 ± 0.03	0.06 ± 0.01	0.41 ± 0.03	2.61 ± 0.49
Foxe Basin	0.49	0.08	0.50	0.86	0.23	0.06	0.41	0.98
Hudson Strait	2.04 ± 0.79	0.08 ± 0.02	0.61 ± 0.09	2.50 ± 1.04	0.53 ± 0.30	0.06 ± 0.01	0.47 ± 0.04	1.12 ± 0.63
2006								
Hudson Bay	2.65 ± 1.41	0.09 ± 0.01	1.05 ± 0.25	4.63 ± 2.17	0.59 ± 0.10	0.07 ± 0.00	0.81 ± 0.22	1.15 ± 0.81
Foxe Basin	2.24	0.13	0.92	3.28	1.09	0.08	0.72	0.76
Hudson Strait	1.90 ± 0.60	0.10 ± 0.01	0.99 ± 0.26	1.79 ± 0.21	0.74 ± 0.15	0.07 ± 0.01	0.82 ± 0.41	0.80 ± 0.79

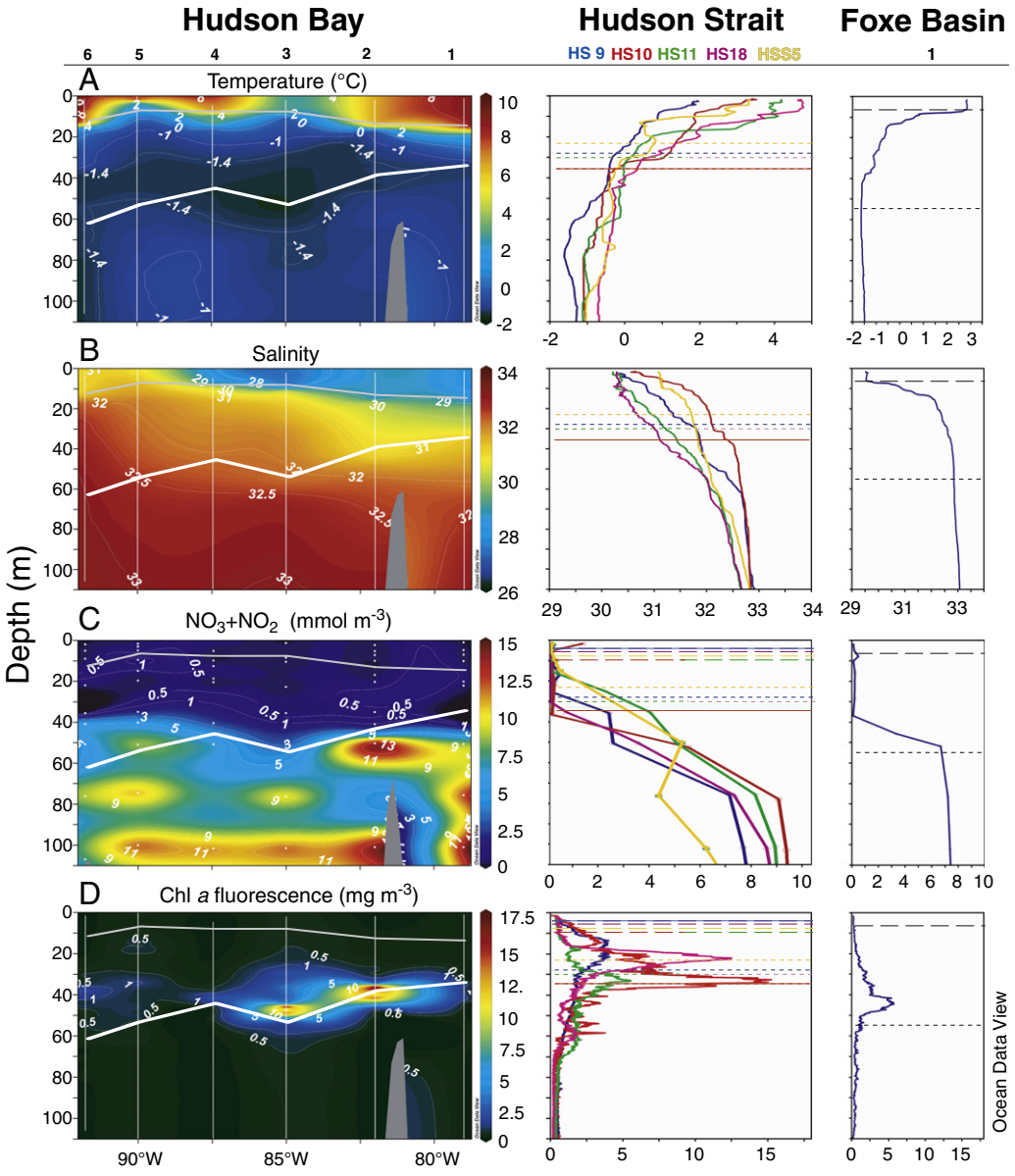

Fig. 2. Spatial distribution of (A) water temperature, (B) salinity, (C) $NO_3 + NO_2$ concentration, and (D) in vivo chlorophyll fluorescence in northern Hudson Bay, Hudson Strait, and Foxe Basin on 2–15 August 2004. Thin gray lines and dashed lines: surface mixed layer depth (Z_m); thick white lines and dotted lines: euphotic zone depth (Z_{eu}). Station locations are shown at the top of the figure.

3.3. Phytoplankton production and biomass

Mean values of phytoplankton production and chl *a* biomass in Z_{eu} were significantly lower in Hudson Bay (0.32 ± 0.14 g C m^{-2} d^{-1} and 30 ± 10 mg chl *a* m^{-2}) than in Hudson Strait (1.15 ± 0.03 g C m^{-2} d^{-1} and 60 ± 30 mg chl *a* m^{-2}) during the three sampling years (Fig. 5). In Foxe Basin, primary production (0.37 ± 0.11 g C m^{-2} d^{-1}) was also significantly lower than the Strait and its phytoplankton biomass (70 ± 30 mg chl *a* m^{-2}) was significantly higher than the Bay. Daily estimated summer primary production averaged 0.32 g C m^{-2} in Hudson Bay and 1.34 g C m^{-2} in Hudson Strait. No year-to-year variability in phytoplankton production or biomass was detected in the HBS during the study period. However, the mean P_T:B_T ratio in the HBS was significantly lower in 2004 (10.5 mg C (mg Chl *a*)$^{-1}$ d^{-1}) and in 2005 (11.3 mg C (mg Chl *a*)$^{-1}$ d^{-1}) than in 2006 (22.3 mg C (mg Chl *a*)$^{-1}$ d^{-1}) (ANOVA, $p<0.05$).

Along the longitudinal transect in Hudson Bay, the maximum phytoplankton production was observed on the western coast in 2004, on the eastern coast in 2005, and on both coasts in 2006 (Fig. 5A–C). In contrast, the chl *a* concentration in Z_{eu} did not show a definite horizontal pattern. Along the north–south transect of Hudson Strait, maximum production rates were recorded at the southern stations in 2005 and 2006 (Fig. 5B, C).

During all sampling periods in Hudson Bay, a DCM was found between 25 and 60 m, usually below the surface mixed layer and at an optical depth of 0.2% of surface irradiance (Figs. 2–4). Maximum phytoplankton production and chl *a* biomass always occurred at shallower depths in the Strait than in the Bay. In the HBS, peaks of primary production occurred above or at the DCM at 61% and 39% of the stations, respectively. In addition, peaks of primary production and chl *a* biomass occurred at Z_{nutr} at 19% and 52% of the stations, respectively. Total phytoplankton abundance at the DCM was statistically higher in 2004 (mean 4635 cells ml^{-1}) than in 2005 (mean 1950 cells ml^{-1}) and 2006 (mean 1508 cells ml^{-1}) in the HBS (ANOVA, $p<0.05$; data not shown).

The percent DOC released during photosynthesis was measured in 2004 and 2005. No year-to-year difference in the percent P_{DOC} contribution to P_{TOC} was detected within Hudson Bay (2004: range

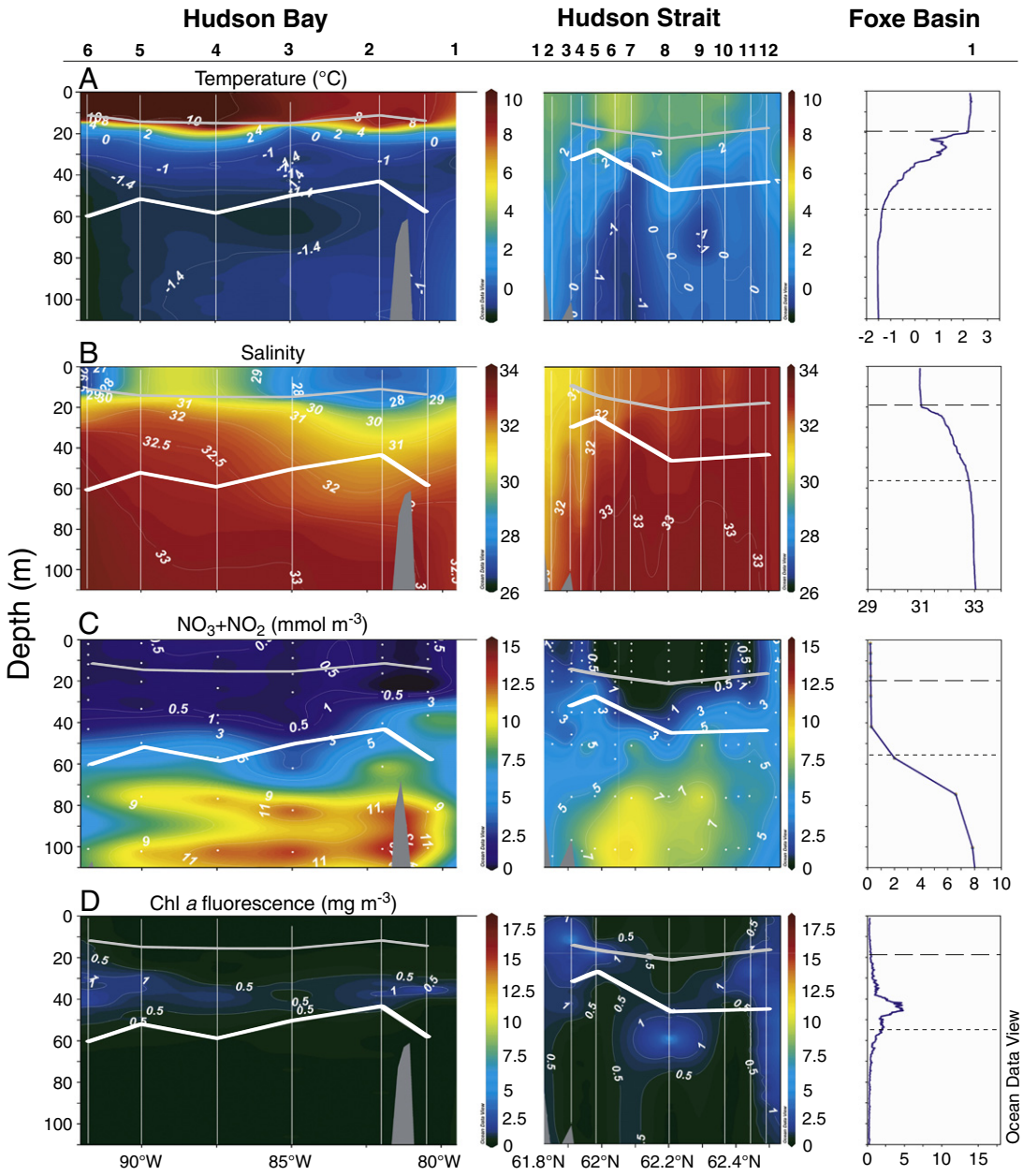

Fig. 3. Spatial distribution of (A) water temperature, (B) salinity, (C) $NO_3 + NO_2$ concentration, and (D) in vivo chlorophyll fluorescence in northern Hudson Bay, Hudson Strait, and Foxe Basin on 1–13 September 2005. Thin gray lines and dashed lines: surface mixed layer depth (Z_m); thick white lines and dotted lines: euphotic zone depth (Z_{eu}). Station locations are shown at the top of the figure.

6.7–18.9%, mean 13.3%; 2005: range 5.6–24.4%, mean 15.3%; *t*-test, $p>0.05$). In contrast, a significantly lower P_{DOC} contribution to P_{TOC} was observed in Hudson Strait in 2004 (range 3.3–6.3%, mean 4.9%) than in 2005 (range 9.3–16.1%, mean 12.1%). A one-way ANOVA showed significant ($p<0.05$) regional differences in 2004, with a higher P_{DOC} contribution to P_{TOC} in Hudson Bay than in Hudson Strait or Foxe Basin.

3.4. Potential fate of primary production and biomass (size fraction)

In the HBS, production was dominated by ultraphytoplankton (0.7–5 µm) except in Hudson Strait and Foxe Basin in 2004 (Fig. 5A–C). However, the chl *a* biomass was dominated by large cells (>5 µm) except for most of Hudson Bay in 2005 (Fig. 5D–E). To illustrate the observed discrepancy between the relative contribution of large-sized phytoplankton biomass to total production in the HBS, we show the variability of the photic-integrated B_L:B_T and P_L:P_T ratios measured during the summers of 2004, 2005, and 2006 in Fig. 6. This figure shows that the contribution of large cells to P_T was smaller than its contribution to B_T, except at stations HB2, HB3, and HB5 in Hudson Bay. In 2004, both small and large cells contributed to the primary production, but large cells dominated the standing stock.

Averaged over the study, diatoms made up more than 40% of the total phytoplankton abundance in the HBS at DCM, except in the central area of the Bay and the northern region of the Strait in 2005 (Fig. 7). Nevertheless, diatoms in the HBS showed a drastic decrease from a relative abundance of 90% in 2004 to 34% in 2005 and 52% in 2006 (Fig. 7). In contrast, the relative and total abundance of dinoflagellates, prymnesiophytes, chrysophytes, cryptophytes and other flagellates all increased from 2004 to 2005–2006 at DCM. This supports the unbalanced contribution of large phytoplankton cells to total production and biomass previously observed in the P:B diagram (Fig. 6).

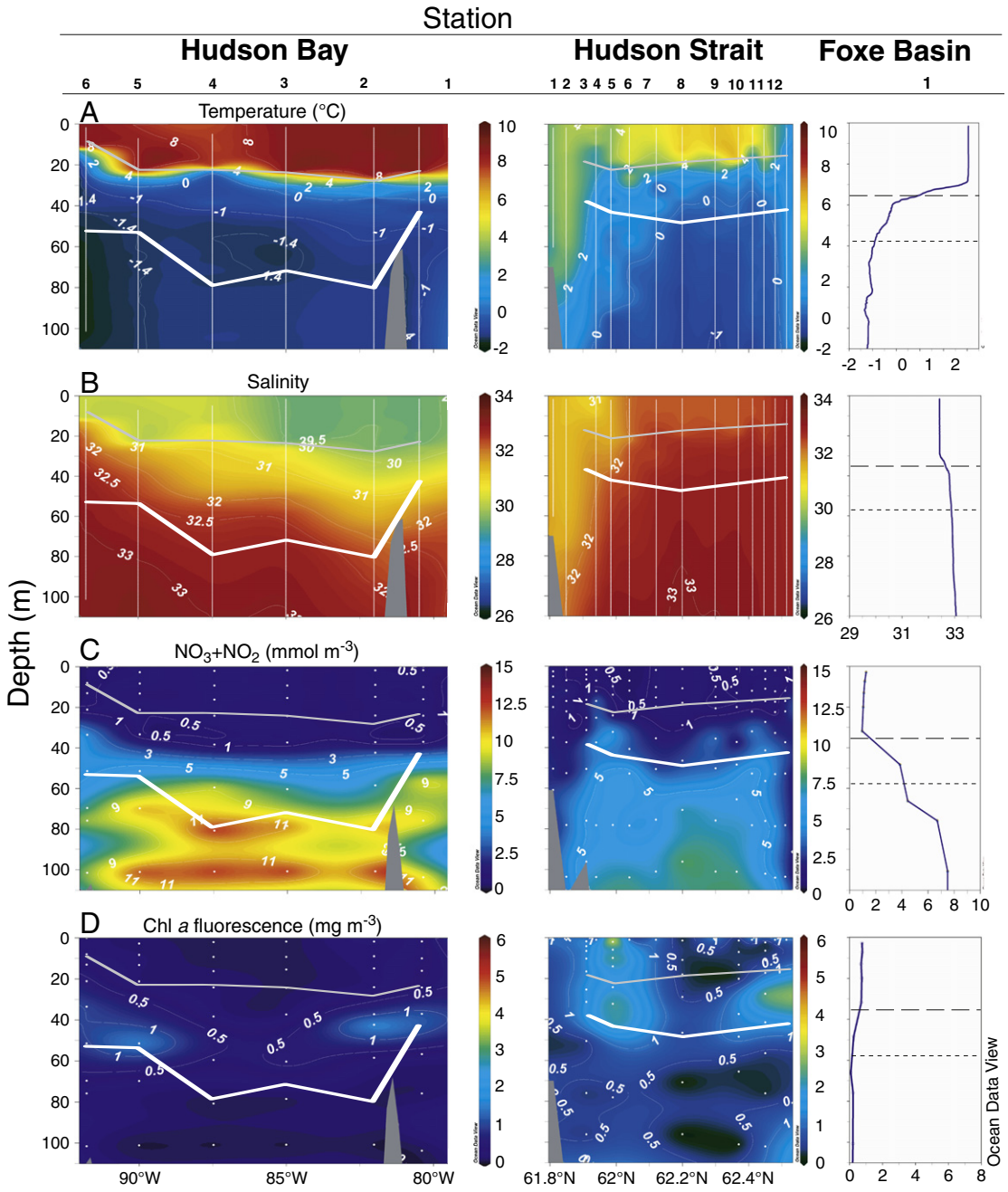

Fig. 4. Spatial distribution of (A) water temperature, (B) salinity, (C) $NO_3 + NO_2$ concentration, and (D) in vivo chlorophyll fluorescence in northern Hudson Bay, Hudson Strait, and Foxe Basin on 30 August–10 September 2006. Thin gray lines and dashed lines: surface mixed layer depth (Z_m); thick white lines and dotted lines: euphotic zone depth (Z_{eu}). Station locations are shown at the top of the figure.

3.5. Environmental control

The two first principal components of the PCA were related to primary production and environmental variables (Fig. 8) and explained 55.8% of the total variance. Principal component 1 (PC1) explained 30.2% of the total variability, and $\Delta\sigma_t$, Z_{nutr}, Z_{eu}, P_T, and B_T contributed the most to this axis. PC2 explained 25.6% of the variance, and this axis was highly correlated with OWDPS, T_{0-Zeu}, Z_m, and E_{0-zeu}. PC1 seems to reproduce the observed spatial pattern in the HBS's phytoplankton production, associating elevated total primary production (P_T) with a low stratification index and shallow Z_{nutr}. Therefore, stations of Hudson Bay and Hudson Strait could be regrouped following their regional trends. PC2 seems to highlight the year-to-year differences by regrouping stations of earlier sampling in 2004 that had higher OWDPS, deeper Z_m, warmer T_{0-zeu}, higher nutrient inventories, and lower light availability in Z_{eu}. As expected from the PCA, a significant negative linear relationship was observed between P_T and the stratification index as well as between P_T and Z_{nutr} for the summers of 2004, 2005, and 2006 (Fig. 9A and B). A statistically significant linear regression also confirmed the positive relationship between P_T and OWDPS in the Bay and in Foxe Basin (Fig. 9C). It should be noted that there were no significant correlations between P_T and the day of the year in the Bay ($r^2 = 0.17$, $p = 0.06$). The euphotic zone depth was negatively correlated with the mean integrated phytoplankton biomass in Z_{eu} ($r^2 = 0.45$, $p < 0.01$), as shown in the PCA results (Fig. 8).

In Hudson Bay, the P_T:B_T ratio was positively correlated with the mean integrated $NO_3 + NO_2$ concentration in Z_{eu} during the three

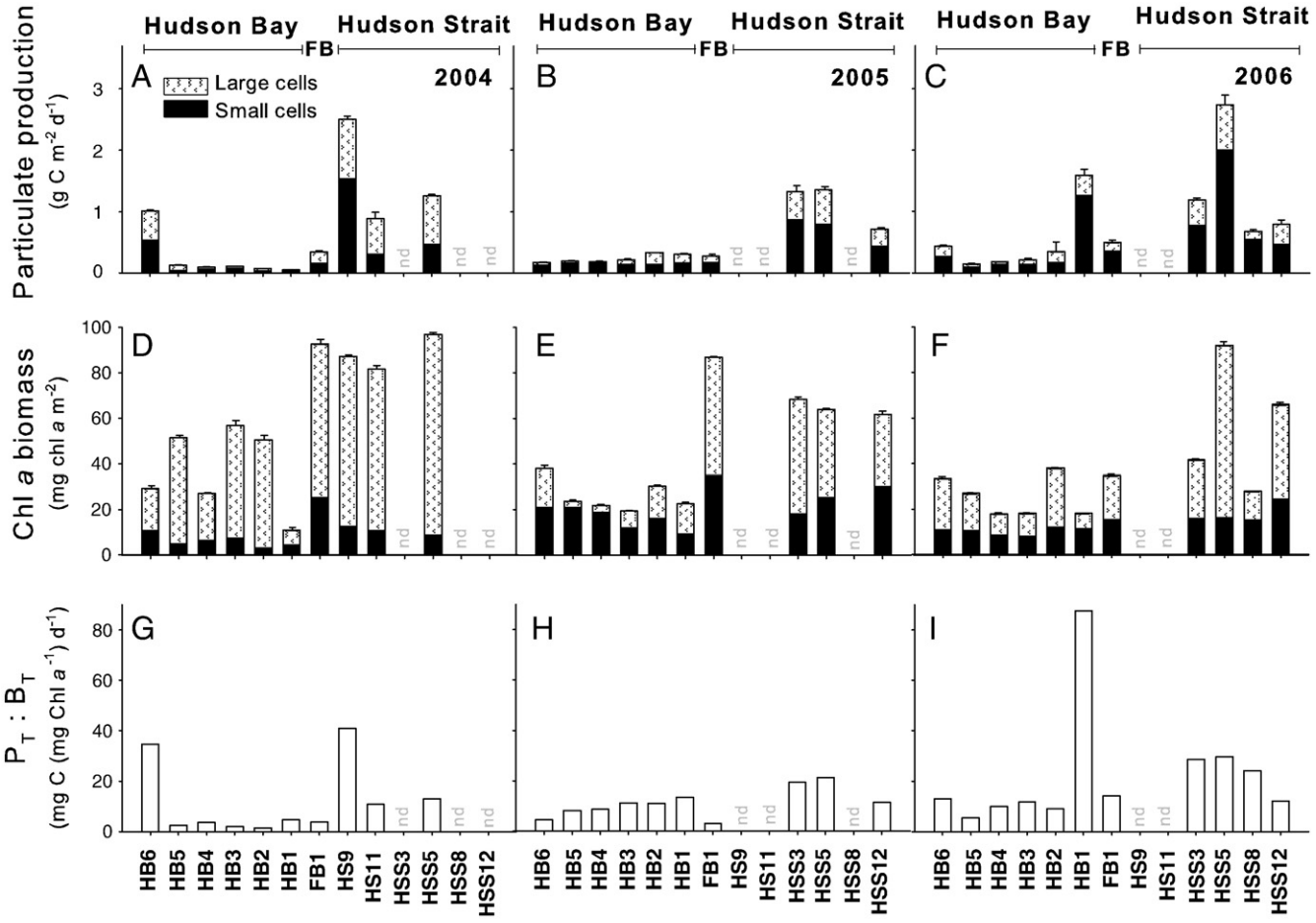

Fig. 5. Spatial variations of (A–C) particulate primary production and (D–F) chlorophyll *a* (chl *a*) biomass for two size fractions (small phytoplankton, 0.7–5 μm; large phytoplankton, ≥5 μm), and (G–I) ratio of particulate primary production to total chl *a* biomass (P_T:B_T) in three regions of the Hudson Bay system in the summers of (A, D, G) 2004, (B, E, H) 2005, and (C, F, I) 2006. Values were depth-integrated from the surface to 0.2% of surface irradiance. In (A–F), bars represent the standard deviations of P_T and B_T. FB: Foxe Basin; nd: no data available.

sampling years ($r^2 = 0.48$, $p < 0.01$). In Hudson Strait, the nitrogen inventory in Z_{eu} was negatively correlated to the strength of the stratification (Fig. 10A); the minimum and maximum stratification indices were observed on the north and south shore, respectively. In addition, P_L, B_L, and the B_L:B_T ratio were also negatively correlated with the nitrogen inventory in Z_{eu} (Fig. 10B–D), and the minimum and maximum $NO_3 + NO_2$ concentrations were always observed on the south and north shores, respectively. These results showed that the maximum values of P_L, B_L, and the B_L:B_T ratio occurred in the depleted nitrogen waters of the south shore.

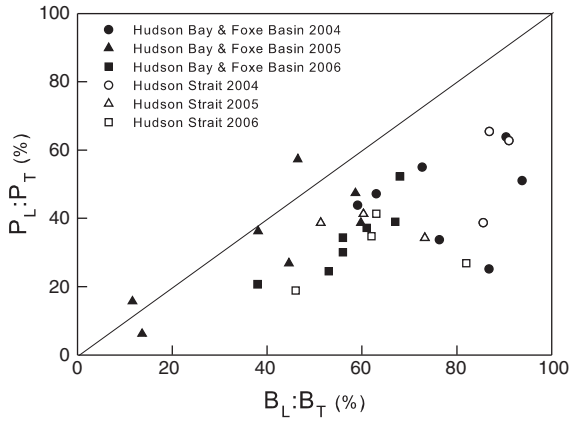

Fig. 6. Production–biomass (P–B) diagram for 31 stations sampled in the Hudson Bay system during the summers of 2004 to 2006. Abscissa: ratio of chlorophyll *a* (chl *a*) biomass of large cells (≥5 μm, B_L) to total chl *a* biomass (≥0.7 μm, B_T); ordinate: ratio of production of large cells (≥5 μm, P_L) to total particulate production (≥0.7 μm, P_T). Values were depth-integrated from the surface to 0.2% of surface irradiance. The main diagonal ($P_L/P_T = B_L/B_T$) corresponds to a balance between production and export for the two size fractions (Tremblay and Legendre, 1994).

4. Discussion

It should be pointed out that this study was conducted in summer, a period characterized by the lightest winds (Maxwell, 1986; Prinsenberg, 1982), the lowest surface layer salinity, and the highest heat flux (Prinsenberg, 1982) of the year in Hudson Bay, as well as a low variability in total freshwater discharge (Déry et al., 2005; Prinsenberg, 1986).

4.1. Spatial variability

In the HBS, two regions were easily distinguished based on phytoplankton production and biomass data: Hudson Bay and Hudson Strait (Figs. 5 and 8). The warmer, less-saline, strongly stratified waters of Hudson Bay were clearly less productive and contained less chl *a* biomass than the colder, saltier, weakly stratified waters of Hudson Strait, as reported previously (Anderson and Roff, 1980a; Drinkwater and Jones, 1987; Harvey et al., 1997). During the three sampling years, phytoplankton production was, on average, 3.6 times

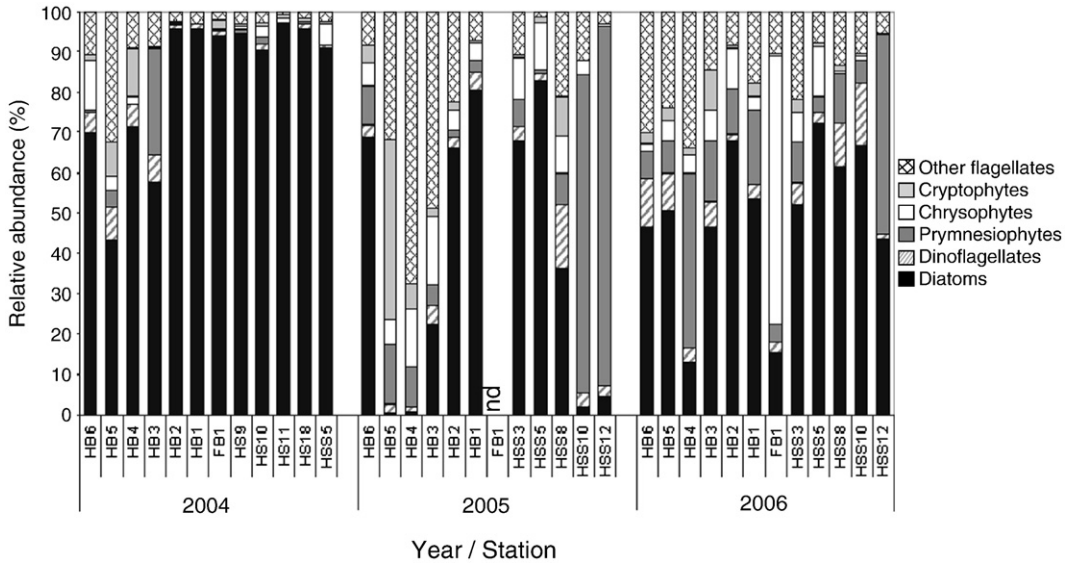

Fig. 7. Relative abundance of the main protist groups at the depths of the chlorophyll fluorescence maxima in the Hudson Bay system during the summers of 2004 to 2006.

lower in Hudson Bay than in Hudson Strait (Fig. 5, Table 4). The Foxe Basin station, located in the southern part of the Basin, showed production rates similar to Hudson Bay but chl *a* biomass similar to Hudson Strait (Figs. 5A, B and 8). Daily primary production rates in Hudson Bay and Foxe Basin were comparable to those of the Beaufort Sea and to the lower range of values reported in the Gulf of St. Lawrence and the Bothnian area of the Baltic Sea (Table 4), two semi-enclosed subarctic seas completely ice covered in winter and ice free in summer (Gagnon and Gough, 2005). In contrast, the higher daily production rates in Hudson Strait were comparable to values of the Chukchi Sea and the North Water area (northern Baffin Bay) in summer (Table 4).

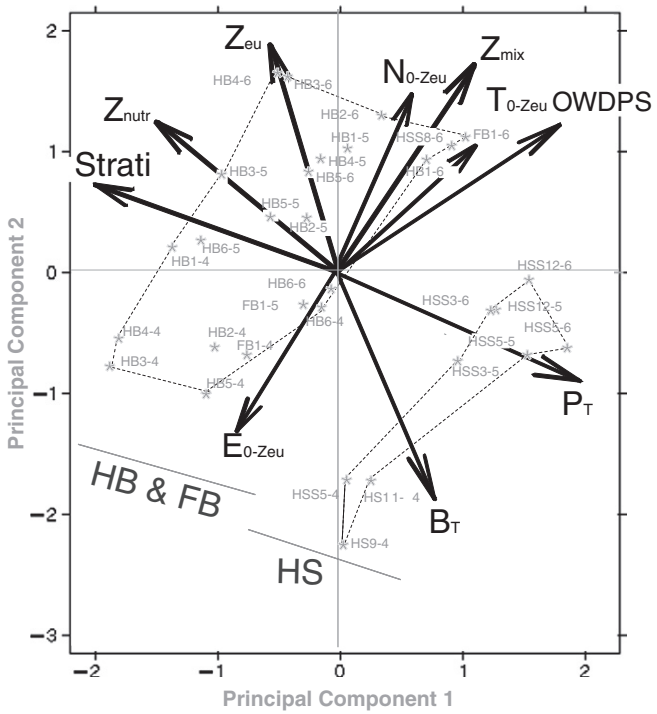

Fig. 8. Principal component analysis of 31 stations sampled in the Hudson Bay system during the summers of 2004 to 2006. The environmental and biological variables are depths of the surface mixed layer (Z_m, m), of the euphotic zone (Z_{eu}, m), and of the nutricline (Z_{nutr}, m); stratification index ($\Delta\sigma_t$); mean irradiance in Z_{eu} ($E_{0\text{-}Zeu}$ mol photons m^{-2} d^{-1}); mean temperature over Z_{eu} ($T_{0\text{-}Zeu}$ °C); open-water days prior to sampling (OWDPS, d); $NO_2 + NO_3$ concentration integrated over Z_{eu} ($N_{0\text{-}Zeu}$ mmol m^{-2}); chlorophyll *a* biomass (B_T, mg m^{-2}) and particulate primary production (P_T, mg C m^{-2} d^{-1}) integrated over Z_{eu}. The dashed lines distinguish stations in Hudson Strait (HS and HSS) from those in Hudson Bay (HB) and Foxe Basin (FB). The numbers 4, 5, and 6 at the end of station abbreviations indicate the sampling year (summers of 2004, 2005, and 2006).

Patterns in phytoplankton production were also observed within Hudson Bay and Hudson Strait. In Hudson Bay, phytoplankton production was generally higher at inshore stations, where diatoms were relatively abundant compared to other phytoplankton groups (Figs. 5 and 7). This general pattern of maximum production rates associated with a diatom-dominated community was also observed in the Northeast Water polynya (northeast Greenland) in spring (Pesant et al., 1996), in the North Water area in spring and fall (Klein et al., 2002), and in the Arctic Ocean in summer (Gosselin et al., 1997).

In Hudson Strait, phytoplankton production was always lower in the cooler, saltier, deeper waters of the north shore compared to the south shore (2005–2006 transect). The lower P_T:B_T and B_L:B_T ratios and the lower phytoplankton production and biomass from large cells in Z_{eu} indicated that the north shore waters did not satisfy bloom conditions, even though nitrogen inventories were higher in these more mixed waters (Drinkwater and Jones, 1987). In contrast to Hudson Bay, the stronger stratification of the south shore stations, generated by higher horizontal advection of fresher water from Hudson Bay and Foxe Basin (Straneo and Saucier, 2008), favored earlier blooms. This follows the classical pattern of a phytoplankton population build-up (Miller, 2004), i.e., a bloom will be initiated only when enriched surface waters are stratified enough to maintain phytoplankton cells in the well-lighted surface water.

Patterns in surface phytoplankton biomass were also highlighted within Hudson Bay and Hudson Strait. In Hudson Bay, surface waters presented a clear inshore–offshore difference in chl *a* concentrations, with values ranging from 0.11 to 0.30 mg m^{-3} (mean 0.20 mg m^{-3}) at inshore stations and from 0.08 to 0.20 mg m^{-3} (mean 0.11 mg m^{-3}) at offshore stations. In Hudson Strait, surface chl *a* concentrations varied between 0.24 and 3.00 mg m^{-3} (mean 1.12 mg m^{-3}) with higher values on the south shore of the Strait (data not shown). Similar concentrations were previously reported for Hudson Bay (Anderson and Roff, 1980a) and Hudson Strait (Drinkwater and Jones, 1987). However, the low surface chl *a* concentrations did not reflect the importance of the phytoplankton biomass present at the bottom of the euphotic zone where summer deep chlorophyll maxima (DCM) consistently formed.

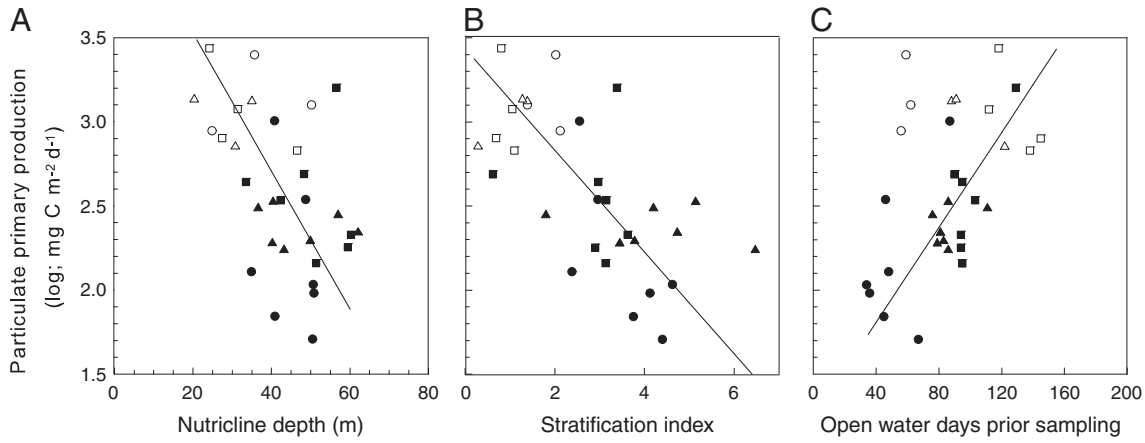

Fig. 9. Relationship between particulate primary production and (A) the depth of the nutricline, (B) the stratification index, and (C) the number of open water days prior to sampling in Hudson Bay and Foxe Basin (black symbols) and Hudson Strait (white symbols) during the summers of 2004 (●,○), 2005 (▲,△), and 2006 (■,□). The regression slopes are shown: (A) $\log_{10}(x_2) = -0.04\ x_1 + 4.35$, $r^2 = 0.25$, $p < 0.0001$; (B) $\log_{10}(x_2) = -0.3\ x_1 + 3.44$, $r^2 = 0.44$, $p < 0.0001$; (C) $\log_{10}(x_2) = 0.01\ x_1 + 1.24$, $r^2 = 0.43$, $p < 0.05$. In (C), only stations from Hudson Bay and Foxe Basin were considered.

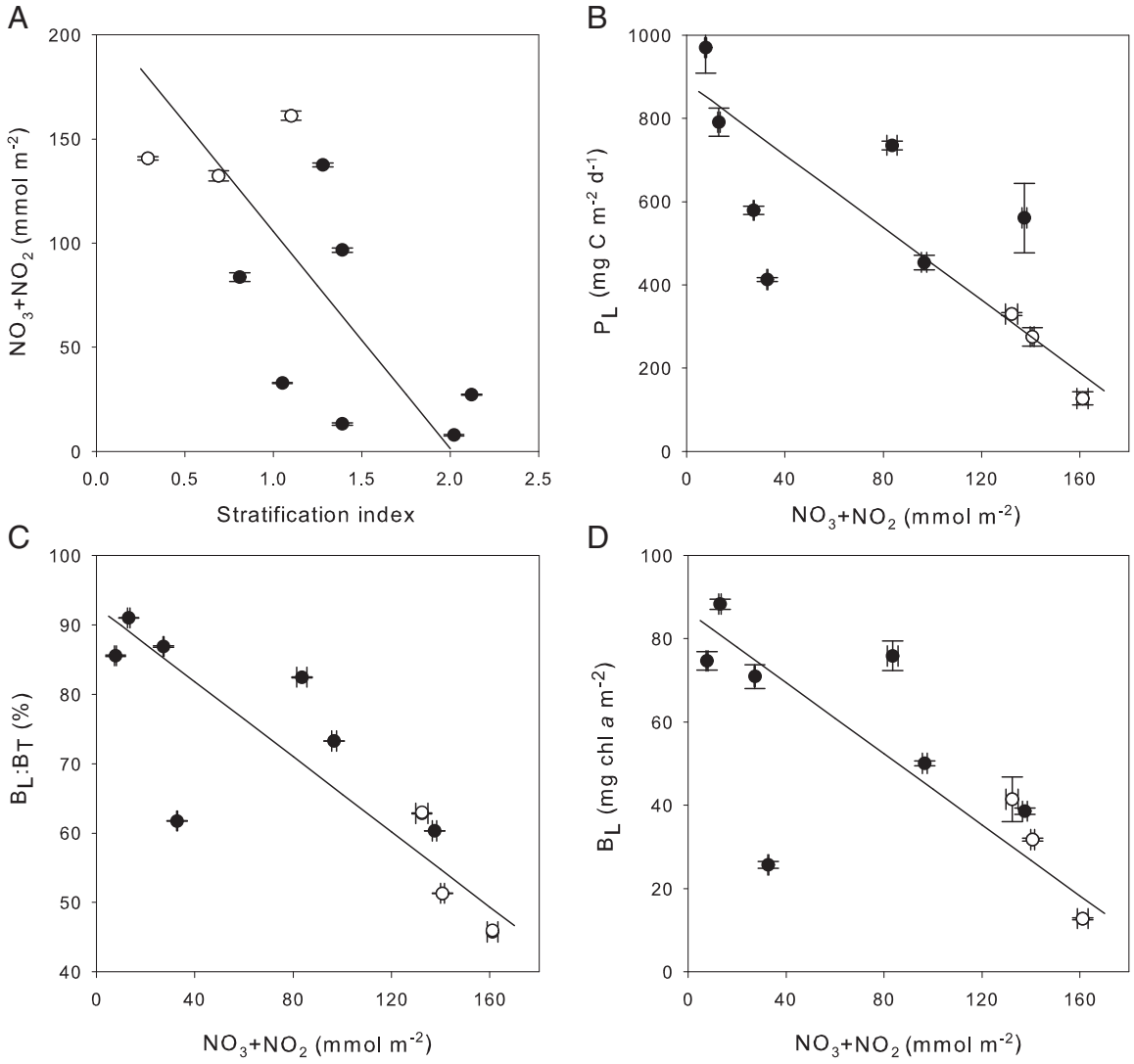

Fig. 10. Relationships between $NO_3 + NO_2$ concentration in the euphotic zone and (A) stratification index, (B) production of large phytoplankton cells (>5 μm, P_L), (C) contribution of large cells to total phytoplankton biomass (B_L:B_T), and (D) biomass of large phytoplankton (B_L) on the south (●) and north (○) shores of Hudson Strait during the summers of 2004–2006. Mean values and standard deviations are shown. The regression slopes are shown: (A) $x_2 = -104.3\ x_1 + 209.9$, $r^2 = 0.44$, $p < 0.05$; (B) $x_2 = -4.36\ x_1 + 886.2$, $r^2 = 0.58$, $p < 0.01$; (C) $x_2 = -0.27\ x_1 + 92.6$, $r^2 = 0.68$, $p < 0.01$; and (D) $x_2 = -0.43\ x_1 + 86.5$, $r^2 = 0.51$, $p < 0.05$.

Table 4
Mean or range of phytoplankton chlorophyll *a* biomass and production in subarctic and arctic seas during summer and fall. nd: no data available.

Location	Lat. (°N)	Chlorophyll *a* (mg m^{-2})	Primary production (mg C m^{-2} d^{-1})	Season	Reference
Arctic					
Beaufort Sea	71	nd	280	Summer	Alexander (1977)[a]
Beaufort Sea	69–71	nd	200	Late July	Carmack et al. (2004)
Beaufort Sea	69–71	nd	40–100	August	Carmack et al. (2004)
Beaufort Sea (Mackenzie shelf)	69–72	16	15–119	Early fall	Brugel et al. (2009)
Beaufort Sea (Amundsen Gulf)	69–72	11	92–105	Late fall	Brugel et al. (2009)
Chukchi/Beaufort Seas (Shelves)	65–75	nd	709	July–August	Walsh et al. (2005)
Chukchi/Beaufort Seas (Shelves)	65–75	nd	578	September–October	Walsh et al. (2005)
Chukchi Sea	70	128	990	Summer	Hameedi (1978)[a]
Chukchi Sea	70–75	25–445	980	July	Gosselin et al. (1997)
Chukchi Sea (Shelf)	70–74	76	783	Summer	Hill and Cota (2005)
Chukchi Sea (Edge Can. Basin)	70–74	35	324	Summer	Hill and Cota (2005)
Deep Canadian Basin	72–77	nd	106	Summer	Lee and Whitledge (2005)
Deep Canadian Basin	76–90	1–25	52	Summer	Gosselin et al. (1997)
Barents Sea (Coastal)	70	31	304	Summer	Yedernikiv and Solov'yeva (1972)[a]
Northern Barents Sea (No bloom)	78–82	nd	43–120	Summer	Hegseth (1998)
Northern Barents Sea (Bloom)	78–82	nd	187–360	Summer	Hegseth (1998)
Pacific					
Mid-subarctic	45–55	nd	150–250	Summer	Koblenz-Mishke (1965)[a]
Mid-subarctic	45–55	21	400	Summer	Larrance (1971)[a]
Bering Sea (Coastal)	55–65	nd	460	Summer	Taguchi (1972)[a]
Bering Sea (Open water)	55–65	nd	330	Summer	Taguchi (1972)[a]
Bering Sea	55–65	nd	340–630	Summer	Taniguchi (1969)[a]
Bering Sea	55–65	76	240	Summer	McRoy et al. (1972)[a]
Atlantic					
Norwegian Sea (Coastal)	69	nd	1120	Summer	Thorndsen and Heimdal (1976)[a]
Baltic Sea (The Sound)	55–56	nd	420–520	Summer	Lassig et al. (1978)
Baltic Proper (Gotland Sea)	54–60	nd	510	Summer	Lassig et al. (1978)
Gulf Finland	59–60	nd	310–680	Summer	Lassig et al. (1978)
Bothnian Sea	61–64	nd	220–280	Summer	Lassig et al. (1978)
Bothnian Bay	64–66	nd	76–140	Summer	Lassig et al. (1978)
E. Greenland (Coastal)	55–70	nd	>350	Summer	Steeman-Nielsen (1958)[a]
E. Greenland (Open water)	55–70	nd	100–200	Summer	Steeman-Nielsen (1958)[a]
Northeast Water polynia	77–81	8–23	212–544	Late Spring–Summer	Pesant et al. (1996)
Gulf of St. Lawrence	46–50	< 22	180–504	Summer–Fall	Tremblay et al. (2000)
Gulf of St. Lawrence	46–50	18	357	Summer–Fall	Savenkoff et al. (2000)
Davis Strait	60	20	21	Summer	MacLaren-Marex, Inc. (1979)[a]
Frobisher Bay	64	100	450	Summer	Grainger (1975)[a]
Baffin Bay	60–76	57	227	Summer	Harrison et al. (1982)[a]
North Water (northern Baffin Bay)	75–79	36–117	845	Late summer	Klein et al. (2002)
North Water (northern Baffin Bay)	75–79	28–47	354	Early fall	Klein et al. (2002)
North Water (northern Baffin Bay)	75–79	57–88	550	Late summer–Early fall	Garneau et al. (2007)
Arctic Canadian Archipelago	75	25	300	Summer	Welch and Kalff (1975)[a]
Hudson Bay system					
Hudson Bay	60	30 (26–38)	320 (236–486)	Summer	This study
Hudson Strait	62	76 (56–87)	1340 (1132–1549)	Summer	This study
Foxe Basin	64	61 (35–87)	370 (279–489)	Summer	This study

[a] Review in Harrison et al. (1982).

Summer DCMs (30–60 m, mean 42 m; Figs. 2–4D) were ubiquitous in the HBS, as reported previously (Anderson and Roff, 1980b; Mundy et al., 2010). In the HBS, DCMs generally occurred near the nutricline—well below the surface mixed layer and generally between 5 and 0.2% of surface irradiance. This implied that the vertical position was driven mainly by a shortage of inorganic nitrogen in the upper Z_{eu}. Similarly, Anderson and Roff (1980b) reported DCMs at ca. 45 m, usually between 0.1 and 1% of surface irradiance in Hudson Bay in August–September 1975. In Hudson Bay, DCMs were never observed at the pycnocline. This DCM feature is typical of stratified oligotrophic waters (Cullen, 1982; Fasham et al., 1985), as observed in Canadian Arctic waters (Carmack et al., 2004; Martin et al., 2010) and in temperate, tropical, and sub-tropical waters (Cullen, 1982; Fasham et al., 1985).

4.2. Nitrogen limitation and stratification

Primary production in the HBS varied negatively with the stratification strength of the upper water column, with lower rates in Hudson Bay than in Hudson Strait. The Hudson Bay upper water column is perennially vertically stable due mainly to buoyancy forces associated with freshwater input from numerous large rivers and seasonal ice melt cycle (Prinsenberg, 1986). This haline stratification restricts upward nutrient flux into the surface layer (Ingram and Prinsenberg, 1998). The weaker stratification in Hudson Strait due to tidal and meteorologically driven mixing (Straneo and Saucier, 2008) probably favored a more regular supply of nutrients in the upper water column. These injected nutrients must have been immediately consumed by phytoplankton, since we did not find any significant difference in surface nutrient concentrations between the Bay and the Strait, except at the north shore stations of the Strait, where phytoplankton seems to be light-limited in the Z_m in summer. Consequently, the strength of stratification limited phytoplankton production and biomass accumulation at most stations of the HBS and clearly differentiated the level of production between the two contrasted hydrodynamic regions of the Bay and the Strait, as hypothesized by Drinkwater and Jones (1987).

In Hudson Bay, NO_3 concentrations in Z_m were within the range of reported values for the half-saturation constant for NO_3 uptake by natural phytoplankton communities ($K_s \leq 1$ mmol m^{-3}; MacIsaac and Dugdale, 1969; Shiomoto et al., 1994). Therefore, it appeared that, prior to our sampling periods, phytoplankton had reduced NO_3 concentrations to levels that limited their production, notably by large cells. It is important to note that Hudson Bay deep waters represent a large nutrient reservoir, with mean concentrations of 12 mmol m^{-3} for nitrate, 30 mmol m^{-3} for silicic acid and 1.7 mmol m^{-3} for phosphate at depths below 100 m (data not shown).

Winter mixing appears to be a critical process to bring nutrient-rich deep water to the surface. Prinsenberg (1986) observed a deepening of the surface mixed layer to at least 90 m at an offshore Hudson Bay station due to surface cooling and salt rejection from freezing ice. This depth was much greater than the nutriclines of 34 to 64 m observed during our summertime study. The thickness of the winter convection layer has been determined an important factor affecting the spring supply of start-up nutrients for primary producers (Lavoie et al., 2008; Plourde and Therriault, 2004) and therefore, total annual primary production (Carmack et al., 2004; Lavoie et al., 2008). This is consistent with the beta-type ocean characteristics described by Carmack (2007), in which permanent stratification, mainly by salinity, constrains the efficiency of nutrient replenishment through winter convection.

Other than vertical mixing, additional nutrient sources can include horizontal advection of water through Fury and Hecla Strait (Prinsenberg, 1986) and from the Baffin Island current (LeBlond et al., 1981), as well as inputs from river runoff (Hudon et al., 1996), ice melt (Freeman et al., 1982), and the atmosphere (Morales-Baquero et al., 2006; Peierls and Paerl, 1997; Pett and Roff, 1982). Furthermore, a source of bioavailable nitrogen generated from break-down of the large pool of dissolved organic matter (DOM) in Hudson Bay surface waters (Granskog et al., 2007; Mundy et al., 2010) could play an important, yet undetermined role on total primary production. Some of these sources could be enhanced by an increasing open water period, thereby helping explain the observed significant relationship between OWDPS and primary production. For example, lengthening of the ice-free season would permit for more wind-induced vertical mixing and horizontal advection events and for longer exposure of the surface DOM to photodegradation (Vähätalo and Järvinen, 2007; Vähätalo and Wetzel, 2004). More nutrient data are needed to provide a complete nitrogen budget for the HBS.

4.3. Temporal variability

In the HBS, there was year-to-year variability in the vertical structure of the water column, notably in the freshwater content of the surface mixed layer and the stratification index, which were higher in 2004–2005 than in 2006, and in the surface mixed layer depth, which gradually increased from 9 m in 2004 to 21 m in 2006. Despite this variability in the hydrographic conditions, there was no year-to-year difference in phytoplankton production and biomass throughout the study period.

However, we observed year-to-year differences in the phytoplankton composition, size structure and physiology. These observations can be summarized by: (1) the contribution of large cells to total phytoplankton biomass and the absolute and relative abundance of diatoms decreased from the mid-summer period sampled in 2004 to the late-summers sampled during 2005–2006; and (2) the P_T:B_T ratio showed an increase from 2004–2005 to 2006.

In mid-summer 2004, formation of the DCM likely resulted from the sinking of an earlier diatom bloom concurrent with depleting concentrations of nutrients, thus reaching a compromise between light and nutrient limitation (Cullen, 1982). This was supported by the dominance of large diatom cells with low photosynthetic performance (i.e., low P_T:B_T ratio) associated with relatively low nutrient concentrations in the upper water column at most stations of the HBS. Therefore, we believe we had observed the decline of a diatom bloom during 2004 from which the onset likely occurred after the ice break-up in late spring, early summer.

From late-summer 2005 to 2006, surface stratification explained variability in the size structure of phytoplankton communities and their mean physiological state (P_T:B_T ratio). During 2006, surface stratification was weaker than 2005, which resulted in a deeper surface mixed layer that was closer to the nutricline and within the euphotic zone. This essentially increased nutrient availability, allowing the growth of healthy large cells (mainly diatoms) ubiquitously throughout the HBS in late-summer 2006. However, the dominance of diatoms at the DCM was much least in late-summers 2005 and 2006 than in mid-summer 2004. This large difference in phytoplankton communities between mid- and late summers may represent a seasonal succession rather than a year-to-year variability.

The apparent year-to-year differences (and absence of differences in production and biomass) need to be confirmed in future work due to possible confounding factors of geographic and/or seasonal variations associated with the limited seasonal coverage of the annual datasets. Nevertheless, the overall results indicate that year-to-year changes in the water column structure had more impact on the composition, cell size, and physiological state of the phytoplankton community than on the total production of the system. This has important implications for the flow of carbon within the ecosystem, since pelagic flagellate-dominated community would lead to longer food chains resulting in inefficient energy transfer to upper trophic levels and low carbon export towards deeper waters compared to diatom-dominated community (Cushing, 1989).

4.4. Estimation of annual phytoplankton production

An estimation of total particulate annual phytoplankton production based on the summers of 2004, 2005, and 2006 gives 39 g C m^{-2} in Hudson Bay, assuming an algal growth season of 120 days. We believe this value was conservative as it does not take into consideration the spring bloom, which was probably associated with the melting ice cover edge (Sibert et al., 2011). Nevertheless, our estimate was similar to the annual phytoplankton production of 35 g C m^{-2} of Roff and Legendre (1986) but lower than the value of 50–70 g C m^{-2} yr^{-1} estimated by Sakshaug (2004) for Hudson Bay.

Even though Hudson Bay is characterized by low annual production, our estimate of 39 g C m^{-2} equates to 24 Mt C yr^{-1} due to its large surface area (620×10^3 km^2, excluding James Bay). Therefore, total areal production in Hudson Bay was higher than that from oligotrophic arctic waters of the Canadian Archipelago (5 Mt C yr^{-1}: Sakshaug, 2004) or the White Sea (2–3 Mt C yr^{-1}; Berger and Primakov, 2007; Sakshaug, 2004) but comparable to the Kara Sea and East Siberian Sea (20–37 and 10–30 Mt C yr^{-1}, respectively; Sakshaug, 2004; Vinogradov et al., 2000).

Hudson Strait had higher annual production rates (161 g C m^{-2}) for a smaller surface area (98×10^3 km^2, excluding Ungava Bay and eastern Hudson Strait), resulting in an estimate of 16 Mt C yr^{-1}. This estimate for Hudson Strait was close to those reported for the Laptev Sea (10–16 Mt C yr^{-1}; Vinogradov et al., 2000; Sakshaug, 2004). The total weighted phytoplankton production for Hudson Bay and Hudson Strait was 55 g C m^{-2} yr^{-1}.

4.5. Potential export

The production–biomass diagram of Tremblay and Legendre (1994) allowed an assessment of the potential fate of phytoplankton carbon produced in Z_{eu}. Our analysis revealed that the contribution of large phytoplankton cells to total production (P_L = 6–66% of P_T, mean 38%) was generally lower than their share of total biomass (B_L = 12–91% of B_T, mean 62%; Fig. 6). This suggests a preferential removal

of small phytoplankton cells by microzooplankton grazing or accumulation of large cells in Z_{eu} (Tremblay and Legendre, 1994). Both interpretations imply that the phytoplankton carbon produced in the HBS was mainly retained in Z_{eu} rather than being exported to depth during our sampling periods.

The potential particulate organic carbon (P_T) export from the euphotic zone (POC_E) was estimated using equations (7) ($POC_E = P_T$ * f-ratio) and (22) (f-ratio $= 0.04 + 0.74\ P_L/P_T$) in Tremblay et al. (1997). For the three sampling years, mean POC_E values were 96 mg C m^{-2} d^{-1} (range: 16–394 mg C m^{-2} d^{-1}) in Hudson Bay, 125 mg C m^{-2} d^{-1} (range: 91–154 mg C m^{-2} d^{-1}) in Foxe Basin, and 441 mg C m^{-2} d^{-1} (range: 121–818 mg C m^{-2} d^{-1}) in Hudson Strait. The values for Hudson Strait were comparable to the POC_E value of 396 mg C m^{-2} d^{-1} estimated for the North Water area in August–September (Klein et al., 2002) and to sinking fluxes estimated from short-term particle interceptor traps of 129–442 mg C m^{-2} d^{-1} at 50 m under open-water conditions in the Chukchi Sea in July–August (Lalande et al., 2007) and of 670 mg C m^{-2} d^{-1}, on average, at 150 m during the decline of the northwest Atlantic spring bloom (Pommier et al., 2008). The POC_E values in Hudson Bay were in agreement with the sinking fluxes of 50–61 mg C m^{-2} d^{-1} at 50 m in Hudson Bay during fall 2005 (Lapoussière et al., 2009) and of 36–67 mg C m^{-2} d^{-1} at 50 m in the Amundsen Gulf during summer (Juul-Pedersen et al., 2010). POC_E values from southern Foxe Basin were comparable to sinking fluxes of 219–240 mg C m^{-2} d^{-1} at 50 m in the North Water polynya in August–September (Caron et al., 2004). For the three years sampled, the total weighted average POC_E for Hudson Bay and Hudson Strait was 17 g C m^{-2} yr^{-1}, making up 31% of the total weighted average primary production in the euphotic zone. The POC_E value was close to the new production value of ca. 24 g C m^{-2} yr^{-1} estimated from total carbonate measurements for northern Hudson Bay (Jones and Anderson, 1994). These results highlight again that most of the organic material produced during the study period in the HBS remained in the euphotic zone, feeding the pelagic system, rather than being exported out of the euphotic zone.

5. Conclusion

This study provides the first measurements of phytoplankton production covering the three hydrographic regions of the HBS (i.e., Hudson Bay, Hudson Strait and Foxe Basin). In addition to confirming the previously documented inshore–offshore gradient in phytoplankton biomass of the surface waters of Hudson Bay (Anderson and Roff, 1980a) and the presence of a subsurface chl *a* maximum at 40–60 m (Anderson and Roff, 1980b), our analysis demonstrated that the waters of Hudson Strait in summer were much more productive than those of northern Hudson Bay and southern Foxe Basin. Furthermore, our study revealed that this large regional variability in phytoplankton production was influenced by the strength of the stratification, which controls the supply of nutrients from deep waters towards the upper water column where phytoplankton are active. The unbalanced contribution of small cells to total production and biomass together with the low POC_E (30% of total production) suggested that the system during the summer to late-summer period likely supports a pelagic dominated food web. Overall, this study revealed a high degree of complexity in primary production and biomass of the HBS and the relationships between these properties and water column structure, which will complicate predictions of how the system will respond to climate change. In that context, there is a crucial need to monitor ocean biology and environmental changes to detect impact of climate change in the HBS. As evidenced by our study, this monitoring should not only measure parameters such as primary production and biomass, but also plankton composition, size structure and physiology.

Acknowledgments

This project was supported by Individual and Northern Research Supplement Discovery grants from the Natural Sciences and Engineering Research Council (NSERC) of Canada to M.G. and by operating grants from the National Centre for Arctic Aquatic Research Excellence (N-CAARE), Department of Fisheries and Oceans Canada, to M.S. J.F. received post-graduate scholarships from the Fonds québécois de la recherche sur la nature et les technologies and the Institut des sciences de la mer de Rimouski (ISMER), and financial support from Indian and Northern Affairs Canada for fieldwork. We thank the officers and crew of the Canadian Coast Guard Ship *Pierre Radisson* for their great support; Mélanie Simard, Liliane St-Amand, Réal Gagnon, Roger Pigeon, Sylvain Cantin, and Michel Harvey for their support before and during the expedition; Sylvie Lessard for phytoplankton analysis; Marie-Lyne Dubé for nutrient analysis; Laure Devine for physical oceanographic data and linguistic revision; Dave Barber for the NSIDC sea-ice cover data; and Christopher-John Mundy, Jean-Éric Tremblay, the Editors Robie Macdonald and Zou Zou Kuzyk, and three anonymous reviewers for their constructive comments on the manuscript. This is a contribution to the research programs of the Department of Fisheries and Oceans Canada (Études des Mers Intérieures du Canada, Hudson Bay northern component [MERICA-nord]), ArcticNet, ISMER, and Québec-Océan.

References

Aagaard, K., Carmack, E.C., 1989. The role of sea ice and other fresh water in the Arctic circulation. J. Geophys. Res. 94, 14485–14498.
ACIA, 2005. Arctic Climate Impact Assessment. Cambridge University Press, Cambridge.
Alexander, V., 1977. Primary productivity regimes of the nearshore Beaufort Sea, with reference to potential roles of ice biota. In: Dunbar, M. (Ed.), Proc. SCOR/SCAR Polar Oceans Conf., Montreal 1974, pp. 609–632.
Anderson, J.T., Roff, J.C., 1980a. Seston ecology of the surface waters of Hudson Bay. Can. J. Fish. Aquat. Sci. 37, 2242–2253.
Anderson, J.T., Roff, J.C., 1980b. Subsurface chlorophyll *a* maximum in Hudson Bay. Nat. Can. 107, 207–213.
Arrigo, K.R., Robinson, D.H., Worthen, D.L., Dunbar, R.B., DiTullio, G.R., VanWoert, M., Lizotte, M.P., 1999. Phytoplankton community structure and the drawdown of nutrients and CO_2 in the Southern Ocean. Science 283, 365–367.
Arrigo, K.R., van Dijken, G., Pabi, S., 2008. Impact of a shrinking Arctic ice cover on marine primary production. Geophys. Res. Lett. 35, L19603. doi:10.1029/2008GL035028.
Barber, F.G., 1967. A contribution to the oceanography of Hudson Bay. Marine Science Branch, Department of Energy, Mines and Resources, Ottawa, Manuscr. Rep. Ser., 4. 69 pp.
Berger, V.Y., Primakov, I.M., 2007. Assessment of primary production in the White Sea. Russ. J. Mar. Biol. 33, 49–53.
Brugel, S., Nozais, C., Poulin, M., Tremblay, J.É., Miller, L.A., Simpson, K.G., Gratton, Y., Demers, S., 2009. Phytoplankton biomass and production in the southeastern Beaufort Sea in autumn 2002 and 2003. Mar. Ecol. Prog. Ser. 377, 63–77.
Canadian Ice Service, Environment Canada, 2009. Graphe des glaces Version 1.0. on-line, dataset http://ice-glaces.ec.gc.ca.
Carmack, E.C., 2007. The alpha/beta ocean distinction: a perspective on freshwater fluxes, convection, nutrients and productivity in high-latitude seas. Deep Sea Res. II 54, 2578–2598.
Carmack, E.C., Macdonald, R.W., Jasper, S., 2004. Phytoplankton productivity on the Canadian Shelf of the Beaufort Sea. Mar. Ecol. Prog. Ser. 277, 37–50.
Caron, G., Michel, C., Gosselin, M., 2004. Seasonal contributions of phytoplankton and fecal pellets to the organic carbon sinking flux in the North Water (northern Baffin Bay). Mar. Ecol. Prog. Ser. 283, 1–13.
Cavalieri, D., Parkinson, C., Gloersen, P., Zwally, H.J., 1996. Sea Ice Concentrations from Nimbus-7 SMMR and DMSP SSM/I Passive Microwave Data, 2004–2006. Digital media, National Snow and Ice Data Center, Boulder, Colorado. (updated 2007).
Comiso, J.C., Nishio, F., 2008. Trends in the sea ice cover using enhanced and compatible AMSR-E, SSM/I, and SMMR Data. J. Geophys. Res. 113, C02S07. doi:10.1029/2007JC004257.
Cullen, J.J., 1982. The deep chlorophyll maximum: comparing vertical profiles of chlorophyll *a*. Can. J. Fish. Aquat. Sci. 39, 791–803.
Cushing, D.H., 1989. A difference in structure between ecosystems in strongly stratified waters and those that are only weakly stratified. J. Plankton Res. 1, 1–13.
Déry, S.J., Stieglitz, M., McKenna, E.C., Wood, E.F., 2005. Characteristics and trends of river discharge into Hudson, James, and Ungava Bays, 1964–2000. J. Clim. 18, 2540–2557.
Drinkwater, K.F., 1986. Physical oceanography of Hudson Strait and Ungava Bay. In: Martini, I.P. (Ed.), Canadian Inland Seas. Elsevier, Amsterdam, pp. 237–264.
Drinkwater, K.F., 1990. Physical and chemical oceanography. In: Percy, J.A. (Ed.), Proceedings of a Workshop: Marine Ecosystem Studies in Hudson Strait, Montréal, 9–10 November 1989: Can. Tech. Rep. Fish. Aquat. Sci. 1770, pp. 87–97.

Drinkwater, K.F., Jones, E.P., 1987. Density stratification, nutrient and chlorophyll distribution in the Hudson Strait region during summer and their relation to tidal mixing. Cont. Shelf Res. 7, 599–607.
Fasham, M.J.R., Platt, T., Irwin, B.D., Jones, K., 1985. Factors affecting the spatial pattern of the deep chlorophyll maximum in the region of the Azores Front. Prog. Oceanogr. 14, 129–165.
Freeman, N.G., Roff, J.C., Pett, R.J., 1982. Physical, chemical and biological features of river plumes under an ice cover in James and Hudson Bays. Nat. Can. 109, 745–764.
Gagnon, A.S., Gough, W.A., 2005. Trends and variability in the dates of freeze-up and break-up over Hudson Bay and James Bay. Arctic 58, 370–382.
Garneau, M.È., Gosselin, M., Klein, B., Tremblay, J.É., Fouilland, E., 2007. New and regenerated production during a late summer bloom in an Arctic polynya. Mar. Ecol. Prog. Ser. 345, 13–26.
Gosselin, M., Levasseur, M., Wheeler, P.A., Horner, R.A., Booth, B.C., 1997. New measurements of phytoplankton and ice algal production in the Arctic Ocean. Deep Sea Res. II 44, 1623–1644.
Grainger, E.H., 1975. A marine ecology study in Frobisher Bay, Arctic Canada. In: Cameron, T.W.M., Billingsly, L.W. (Eds.), Energy flow - its biological dimensions, a summary of the IBP in Canada, 1964–1974. Royal Society of Canada, Ottawa, pp. 261–266.
Grainger, E.H., 1982. Factors affecting phytoplankton stocks and primary productivity at the Belcher Islands, Hudson Bay. Nat. Can. 109, 787–791.
Granskog, M.A., Macdonald, R.W., Mundy, C.J., Barber, D.G., 2007. Distribution, characteristics and potential impacts of chromophoric dissolved organic matter (CDOM) in Hudson Strait and Hudson Bay, Canada. Cont. Shelf Res. 27, 2032–2050.
Grebmeier, J.M., Cooper, L.W., Feder, H.M., Sirenko, B.I., 2006. Ecosystem dynamics of the Pacific-influenced Northern Bering and Chukchi Seas in the Amerasian Arctic. Prog. Oceanogr. 71, 331–361.
Hameedi, M.J., 1978. Aspects of water column primary productivity in the Chukchi Sea during summer. Mar. Biol. 48, 37–46.
Harrison, W., Platt, T., Irwin, B., 1982. Primary production and nutrient assimilation by natural phytoplankton populations of the eastern Canadian Arctic. Can. J. Fish. Aquat. Sci. 39, 335–345.
Harvey, M., Therriault, J.C., Simard, N., 1997. Late-summer distribution of phytoplankton in relation to water mass characteristics in Hudson Bay and Hudson Strait (Canada). Can. J. Fish. Aquat. Sci. 54, 1937–1952.
Harvey, M., Therriault, J.C., Simard, N., 2001. Hydrodynamic control of late summer species composition and abundance of zooplankton in Hudson Bay and Hudson Strait (Canada). J. Plankton Res. 23, 481–496.
Harvey, M., Starr, M., Therriault, J.C., Saucier, F., Gosselin, M., 2006. MERICA-nord program: monitoring and research in the Hudson Bay complex. Atl. Zone Monit. Prog. AZMP Bull. 5, 27–32.
Hegseth, E.N., 1998. Primary production in the northern Barents Sea. Polar Res. 17, 113–123.
Hill, V., Cota, G., 2005. Spatial patterns of primary production on the shelf, slope and basin of the Western Arctic in 2002. Deep-Sea Res. II 52, 3344–3354.
Hochheim, K.P., Barber, D.G., 2010. Atmospheric forcing of sea ice in Hudson Bay during the fall period, 1980–2005. J. Geophys. Res. 115, C05009. doi:10.1029/2009JC005334.
Hochheim, K.P., Lukovich, J.V., Barber, D.G., 2011. Atmospheric forcing of sea ice in Hudson Bay during the spring period: 1980–2005. J. Mar. Syst. 88, 476–487.
Holmes, W.R., 1970. The Secchi disk in turbid coastal waters. Limnol. Oceanogr. 15, 688–694.
Hudon, C., Morin, R., Bunch, J., Harland, R., 1996. Carbon and nutrient output from the Great Whale River (Hudson Bay) and a comparison with other rivers around Quebec. Can. J. Fish. Aquat. Sci. 53, 1513–1525.
Ingram, R.G., Prinsenberg, S., 1998. Coastal oceanography of Hudson Bay and surrounding Eastern Canadian Arctic Waters. In: Robinson, A.R., Brink, K.N. (Eds.), The Sea, vol 11. Wiley, pp. 835–861.
IPCC, 2007. Climate change 2007: The physical science basis. Contribution of Working Group I to the Fourth Assessment Report of the Intergovernmental Panel on Climate Change. Cambridge University Press, Cambridge, UK.
Johannessen, O.M., Bengtsson, L., Miles, M.W., Kuzmina, S.I., Semenov, V.A., Alekseev, G.V., Nagurnyi, A.P., Zakharov, V.F., Bobylev, L.P., Petersson, L.H., Hasselmann, K., Cattle, H.P., 2004. Arctic climate change: observed and modelled temperature and sea-ice variability. Tellus A 56, 559–560.
Jones, E.P., Anderson, L.G., 1994. Northern Hudson Bay and Foxe Basin—water masses, circulation and productivity. Atmos. Ocean 32, 361–374.
Juul-Pedersen, T., Michel, C., Gosselin, M., 2010. Sinking export of particulate organic material from the euphotic zone in the eastern Beaufort Sea. Mar. Ecol. Prog. Ser. 410, 55–70.
Klein, B., LeBlanc, B., Mei, Z.P., Béret, R., Michaud, J., Mundy, C.J., von Quillfeldt, C.H., Garneau, M.È., Roy, S., Gratton, Y., Cochran, J.K., Bélanger, S., Larouche, P., Pakulski, J.D., Rivkin, R.B., Legendre, L., 2002. Phytoplankton biomass, production and potential export in the North Water. Deep Sea Res. II 49, 4983–5002.
Knap, A., Michaels, A., Close, A., Ducklow, H., Dickson, A., 1996. Protocols for the Joint Global Ocean Flux Study (JGOFS) core measurements. JGOFS Report No. 19. Reprint of the IOC Manual and Guides No 29, UNESCO, 1994.
Koblenz-Mishke, O.I., 1965. Primary production in the Pacific. Oceanology 5, 104–116.
Kwok, R., Cunningham, G.F., Wensnahan, M., Rigor, I., Zwally, H.J., Yi, D., 2009. Thinning and volume loss of the Arctic sea ice cover: 2003–2008. J. Geophys. Res. 114, C07005. doi:10.1029/2009JC005312.
Lalande, C., Grebmeier, J.M., Wassmann, P., Cooper, L.W., Flint, M.V., Sergeeva, V.M., 2007. Export fluxes of biogenic matter in the presence and absence of seasonal sea ice cover in the Chukchi Sea. Cont. Shelf Res. 27, 2051–2065.
Lapoussière, A., Michel, C., Gosselin, M., Poulin, M., 2009. Spatial variability in organic material sinking export in the Hudson Bay system, Canada, during fall. Cont. Shelf Res. 29, 1276–1288.
Larrance, T.D., 1971. Primary production in the mid-subarctic Pacific region, 1966–1968. Fish. Bull. 69, 595–613.
Lassig, J., Leppänen, J.M., Niemi, Å., Tammelander, G., 1978. Phytoplankton primary production in 1972–1975, as compared with other parts of the Baltic Sea. Finn. Mar. Res. 244, 101–115.
Lavoie, D., Macdonald, R.W., Denman, K.L., 2008. Primary productivity and export fluxes on the Canadian shelf of the Beaufort Sea: a modelling study. J. Mar. Syst. 75, 17–32.
Lean, D.R.S., Burnison, B.K., 1979. An evaluation of errors in the ^{14}C method of primary production measurement. Limnol. Oceanogr. 24, 917–938.
LeBlond, P.H., Osborn, T.R., Hodgins, D.O., Goodman, R., Metge, M., 1981. Surface circulation of the western Labrador Sea. Deep Sea Res. 28, 683–693.
Lee, S.H., Whitledge, T.E., 2005. Primary and new production in the deep Canada Basin. Polar Biol. 28, 190–197.
Legendre, L., LeFèvre, J., 1989. Hydrodynamical singularities as controls of recycled versus export production in oceans. In: Berger, W.H., Smetacek, V.S., Wefer, G. (Eds.), Productivity of the Ocean: Present and Past. Wiley, Chichester, pp. 49–63.
Legendre, L., Simard, Y., 1979. Océanographie biologique estivale et phytoplancton dans le sud-est de la baie d'Hudson. Mar. Biol. 52, 11–22.
Legendre, L., Demers, S., Yentsch, C.M., Yentsch, C.S., 1983. The ^{14}C method: patterns of dark CO_2 fixation and DCMU correction to replace the dark bottle. Limnol. Oceanogr. 28, 996–1003.
Li, W.K.W., Irwin, B.D., Dickie, P.M., 1993. Dark fixation of ^{14}C: variations related to biomass and productivity of phytoplankton and bacteria. Limnol. Oceanogr. 38, 483–494.
Lorbacher, K., Dommenget, D., Niiler, P.P., Köhl, A., 2006. Ocean mixed layer depth: a subsurface proxy of ocean–atmosphere variability. J. Geophys. Res. 111, C07010. doi:10.1029/2003JC002157.
Lund, J.W.G., Kipling, C., Le Cren, E.D., 1958. The inverted microscope method of estimating algal numbers and the statistical basis of estimations by counting. Hydrobiologia 11, 143–170.
MacIsaac, J.J., Dugdale, R.C., 1969. The kinetics of nitrate and ammonia uptake by natural populations of marine phytoplankton. Deep Sea Res. 16, 45–57.
MacLaren-Marex, Inc, 1979. Primary productivity studies in the water column and pack ice of the Davis Strait, April, May and August 1978. Report, Indian and Northern Affairs, Canada.
Mann, K.H., Lazier, J.R.N., 1996. Dynamics of Marine Ecosystems: Biological–Physical Interactions in the Oceans. Blackwell Scientific Publications, Boston.
Martin, J., Tremblay, J.-É., Gagnon, J., Tremblay, G., Lapoussière, A., Jose, C., Poulin, M., Gosselin, M., Gratton, Y., Michel, C., 2010. Prevalence, structure and properties of subsurface chlorophyll maxima in Canadian Arctic waters. Mar. Ecol. Prog. Ser. 412, 69–84.
Maxwell, J.B., 1986. A climate overview of the Canadian inland seas. In: Martini, I.P. (Ed.), Canadian Inland Seas. Elsevier, Amsterdam, pp. 79–116.
McClelland, J.W.J., Déry, S.J., Peterson, B.J., Holmes, R.M., Wood, E.F., 2006. A pan-arctic evaluation of changes in river discharge during the latter half of the 20th century. Geophys. Res. Lett. 33, L06715. doi:10.1029/2006GL025753.
McRoy, C.P., Goering, J.J., Shiels, W.S., 1972. Studies of primary productivity in the eastern Bering Sea. In: Takenouti, A.Y. (Ed.), Biological oceanography of the northern North Pacific Ocean. Idemitsu Shoten, Tokyo, pp. 199–216.
Melling, H., Agnew, T.A., Falkner, K.K., Greenberg, D.D., Lee, C.M., Münchow, A., Petrie, B., Prinsenberg, S.J., Samelson, R.M., Woodgate, R.A., 2008. Fresh-water fluxes via Pacific and Arctic outflows across the Canadian Polar shelf. In: Dickson, R.R., Meincke, J., Rhines, P. (Eds.), Arctic–Subarctic Ocean Fluxes: Defining the Role of the Northern Seas in Climate. Springer Science + Business Media B.V., Dordrecht, The Netherlands, pp. 193–247.
Miller, C.B., 2004. Biological Oceanography. Blackwell Publishing, Malden, MA.
Mingelbier, M., Klein, B., Claereboudt, M.R., Legendre, L., 1994. Measurement of daily primary production using 24 h incubations with the ^{14}C method: a caveat. Mar. Ecol. Prog. Ser. 113, 301–309.
Mitchell, M.R., Harrison, G., Pauley, K., Gagné, A., Maillet, G., Strain, P., 2002. Atlantic zonal monitoring program sampling protocol. Can. Tech. Rep. Hydrogr. Ocean. Sci. 223 (iv + 23 pp.).
Moline, M.A., Karnovsky, N.J., Brown, Z., Divoky, G.J., Frazer, T.K., Jacoby, C.A., Torres, J.J., Fraser, W.R., 2008. High latitude changes in ice dynamics and their impact on polar marine ecosystems. Ann. N.Y. Acad. Sci. 1134, 267–319.
Morales-Baquero, R., Pulido-Villena, E., Reche, I., 2006. Atmospheric inputs of phosphorus and nitrogen to the southwest Mediterranean region: biogeochemical responses of high mountain lakes. Limnol. Oceanogr. 51, 830–837.
Mundy, C.J., Gosselin, M., Starr, M., Michel, C., 2010. Riverine export and the effects of circulation on dissolved organic carbon in the Hudson Bay system, Canada. Limnol. Oceanogr. 55, 315–323.
Parsons, T.R., Maita, Y., Lalli, C.M., 1984. A Manual of Chemical and Biological Methods for Seawater Analysis. Pergamon Press, Toronto.
Peierls, B.L., Paerl, H.W., 1997. Bioavailability of atmospheric organic nitrogen deposition to coastal phytoplankton. Limnol. Oceanogr. 42, 1819–1823.
Pesant, S., Legendre, L., Gosselin, M., Smith, R.E.H., Kattner, G., Ramseier, R.O., 1996. Size-differential regimes of phytoplankton production in the Northeast Water Polynya (77°–81°N). Mar. Ecol. Prog. Ser. 142, 75–86.
Peterson, B.J., McClelland, J., Curry, R., Holmes, R.M., Walsh, J.E., Aagaard, K., 2006. Trajectory shifts in the Arctic and subarctic freshwater cycle. Science 313, 1061–1066.
Pett, R.J., Roff, J.C., 1982. Some observations and deductions concerning the deep water of Hudson Bay. Nat. Can. 109, 767–774.

Plourde, J., Therriault, J.-C., 2004. Climate variability and vertical advection of nitrates in the Gulf of St. Lawrence, Canada. Mar. Ecol. Prog. Ser. 279, 33–43.
Pommier, J., Michel, C., Gosselin, M., 2008. Particulate organic carbon export in the upper twilight zone of the northwest Atlantic Ocean during the decline of the spring bloom. Mar. Ecol. Prog. Ser. 356, 81–92.
Pommier, J., Gosselin, M., Michel, C., 2009. Size-fractionated phytoplankton production and biomass during the decline of the northwest Atlantic spring bloom. J. Plankton Res. 31, 429–446.
Post, É., Forchhammer, M.C., Syndonia Bret-Harte, M., Callaghan, T.V., Christensen, T.R., Elberling, B., Fox, A.D., Gilg, O., Hik, D.S., Høye, T.T., Ims, R.A., Jeppesen, E., Klein, D.R., Madsen, J., McGuire, A.D., Rysgaard, S., Schindler, D.E., Stirling, I., Tamstorf, M.P., Tyler, N.J.C., van der Wal, R., Welker, J., Wookey, P.A., Schmidt, N.M., Aastrup, P., 2009. Ecological dynamics across the Arctic associated with recent climate change. Science 325, 1355–1358.
Prinsenberg, S.J., 1977. Freshwater budget of Hudson Bay. Ocean Aquat. Sci. Cent. Reg. M.S. Rep. Ser., 5. 71 pp.
Prinsenberg, S.J., 1980. Man-made changes in freshwater input rates of Hudson and James Bays. Can. J. Fish. Aquat. Sci. 37, 1101–1111.
Prinsenberg, S.J., 1982. Time variability of physical oceanographic parameters in Hudson Bay. Nat. Can. 109, 685–700.
Prinsenberg, S.J., 1984. Freshwater contents and heat budgets of James Bay and Hudson Bay. Cont. Shelf Res. 3, 191–200.
Prinsenberg, S.J., 1986. The circulation pattern and current structure of Hudson Bay. In: Martini, I.P. (Ed.), Canadian Inland Seas. Elsevier, Amsterdam, pp. 187–204.
Redfield, A.C., Ketchum, B.H., Richards, F.A., 1963. The influence of organisms on the composition of sea water. In: Hill, M.N. (Ed.), The Sea, Vol. 2. Interscience, New York, pp. 26–77.
Riley, G.A., 1957. Phytoplankton of the north central Sargasso Sea, 1950–52. Limnol. Oceanogr. 2, 252–270.
Roff, J.C., Legendre, L., 1986. Physico-chemical and biological oceanography of Hudson Bay. In: Martini, I.P. (Ed.), Canadian Inland Seas. Elsevier, Amsterdam, pp. 265–291.
Sakshaug, E., 2004. Primary and secondary production in the Arctic Seas. In: Stein, R., Macdonald, R.W. (Eds.), The Organic Carbon Cycle in the Arctic Ocean. Springer-Verlag, Berlin-Heidelberg, pp. 57–81.
Saucier, F.J., Senneville, S., Prinsenberg, S., Roy, F., Smith, G., Gachon, P., Caya, D., Laprise, R., 2004. Modelling the sea ice-ocean seasonal cycle in Hudson Bay, Foxe Basin and Hudson Strait, Canada. Clim. Dyn. 23, 303–326.
Savenkoff, C., Vézina, A.F., Roy, S., Klein, B., Lovejoy, C., Therriault, J.C., Legendre, L., Rivkin, R., Bérubé, C., Tremblay, J.É., Silverberg, N., 2000. Export of biogenic carbon and structure and dynamics of the pelagic food web in the Gulf of St. Lawrence. I. Seasonal variations. Deep-Sea Res. II 47, 585–607.
Schlitzer, R., 2004. Ocean Data View. http://odv.awi.de.
Shiklomanov, I.A., Shiklomanov, A.I., Lammers, R.B., Peterson, B.J., Vorosmarty, C.J., 2000. The dynamics of river water inflow to the Arctic Ocean. In: Lewis, L.E., Jones, E.P., Prowse, T.D., Wadhams, P. (Eds.), The Freshwater Budget of the Arctic Ocean. Kluwer Academic, Dordrecht, The Netherlands, pp. 281–296.
Shiomoto, A., Sasaki, K., Shimoda, T., Matsumura, S., 1994. Kinetics of nitrate and ammonium uptake by natural population of marine phytoplankton in the surface water of the Oyashio region during spring and summer. J. Oceanogr. 50, 515–529.
Sibert, V., Zakardjian, B., Gosselin, M., Starr, M., Senneville, S., LeClainche, Y., 2011. 3D bio-physical model of the sympagic and planktonic productions in the Hudson Bay system. J. Mar. Syst. 88, 401–422.
Smetacek, V., Nicol, S., 2005. Polar ocean ecosystems in a changing world. Nature 437, 362–368.
Smith, J.C., Platt, T., Li, W.K.W., Horne, E.P.W., Harrison, W.G., Subba Rao, D.V., Irwin, B.D., 1985. Arctic marine photoautotrophic picoplankton. Mar. Ecol. Prog. Ser. 20, 207–220.
Smith Jr., W.O., Gosselin, M., Legendre, L., Wallace, D.W.R., Daly, K.L., Kattner, G., 1997. New production in the Northeast Water Polynya: 1993. J. Mar. Syst. 10, 199–209.
Sokal, R.R., Rohlf, F.J., 1995. Biometry: The Principles and Practice of Statistics in Biological Research, 3nd ed. W.H. Freeman, New York.
Steeman-Nielsen, E., 1958. A survey of recent Danish measurements of the organic productivity in the sea. Rapp. Cons. Explor. Mer. 144, 92–95.
Steward, D.B., Lockhart, W.L., 2005. An overview of the Hudson Bay marine ecosystem. Can. Tech. Rep. Fish. Aquat. Sci. 2586 (487 pp.).
Straneo, F., Saucier, F., 2008. The outflow from Hudson Strait and its contribution to the Labrador Current. Deep Sea Res. I 55, 926–946.
Stroeve, J., Holland, M.M., Meier, W., Scambos, T., Serreze, M., 2007. Arctic sea-ice decline: faster than forecast. Geophys. Res. Lett. 34, L09501. doi:10.1029/2007GL029703.
Subba Rao, D.V., Platt, T., 1984. Primary production in Arctic waters. Polar Biol. 3, 191–201.
Taguchi, S., 1972. Mathematical analysis of primary production in the Bering Sea in summer. In: Takenouti, A.Y. (Ed.), Biological oceanography of the northern North Pacific Ocean. Idemitsu Shoten, Tokyo, pp. 253–262.
Taniguchi, A., 1969. Regional variations of surface primary production in the Bering Sea in summer and the vertical stability of water affecting the production. Bull. Fac. Fish. Hokkaido Univ. 20, 169–179.
Thorndsen, J., Heimdal, B.R., 1976. Primary production, phytoplankton and light in Straumsbukta near Troms. Astarte 9, 51–60.
Tremblay, J.É., Legendre, L., 1994. A model for the size-fractionated biomass and production of marine phytoplankton. Limnol. Oceanogr. 39, 2004–2014.
Tremblay, J.É., Klein, B., Legendre, L., Rivkin, R.B., Therriault, J.C., 1997. Estimation of *f*-ratios in oceans based on phytoplankton size structure. Limnol. Oceanogr. 42, 595–601.
Tremblay, J.É., Legendre, L., Klein, B., Therriault, J.C., 2000. Size-differential uptake of nitrogen and carbon in a marginal sea (Gulf of St. Lawrence, Canada): significance of diel periodicity and urea uptake. Deep-Sea Res. II 47, 489–518.
Tritton, D.J., 1988. Physical Fluid Dynamics, 2nd ed. Clarendon Press, Oxford.
Vähätalo, A.V., Järvinen, M., 2007. Photochemically produced bioavailable nitrogen from biologically recalcitrant dissolved organic matter stimulates production of a nitrogen-limited microbial food web in the Baltic Sea. Limnol. Oceanogr. 52, 132–143.
Vähätalo, A.V., Wetzel, R.G., 2004. Photochemical and microbial decomposition of chromophoric dissolved organic matter during long (months–years) exposures. Mar. Chem. 89, 313–326.
Vinogradov, M.E., Vedernikov, V.I., Romankevich, E.A., Vetrov, A.A., 2000. Components of the carbon cycle in the Russian Arctic Seas: primary production and flux of C-org from the photic layer. Oceanology 40, 204–215.
Walsh, J.E., 2009. A comparison of Arctic and Antarctic climate change, present and future. Antarct. Sci. 21, 179–188.
Walsh, J.J., Dieterle, D.A., Maslowski, W., Grebmeier, J.M., Whitledge, T.E., Flint, M., Sukhanova, I.N., Bates, N., Cota, G.F., Stockwell, D., Moran, S.B., Hansell, D.A., McRoyd, C.P., 2005. A numerical model of seasonal primary production in the Chuckchi/Beaufort Seas. Deep Sea Res. II 52, 3541–3576.
Wang, M., Overland, J.E., 2009. A sea ice free summer arctic within 30 years? Geophys. Res. Lett. 36, L07502. doi:10.1029/2009GL037820.
Welch, H.E., Kalff, J., 1975. Marine metabolism at Resolute Bay. Northwest Territories. Proc. Circumpolar Conf. on Northern Ecology. Nat. Res. Counc., Ottawa. pp. 69–75.
Yedernikiv, V.I., Solov'yeva, A.A., 1972. Primary production and chlorophyll in the coastal waters of the Barents Sea. Oceanology 12, 559–565.
Ziegler, A.D., Sheffield, J., Maurer, E.P., Nijssen, B., Wood, E.F., Lettenmaier, D.P.L., 2003. Detection of intensification in global- and continental-scale hydrological cycles: temporal scale of evaluation. J. Clim. 16, 535–547.